Alexandra Kuznetsova

Licenciada

STOCHASTIC SIMULATION OF THE MORPHOLOGY OF FLUVIAL SAND CHANNELS RESERVOIRS

Dissertação para obtenção do Grau de Mestre em Engenharia Geológica

(Georrecursos)

Orientador: Doutor José António de Almeida, Prof. Auxiliar – FCT/UNL

Co-orientador: Doutor Paulo Alexandre Rodrigues Roque Legoinha, Prof. Auxiliar – FCT/UNL

Júri:

Presidente: Doutor José Carlos Ribeiro Kullberg, Prof. Auxiliar – FCT/UNL

Vogais:Doutora Júlia Cristina da Costa Carvalho, Investigadora. Auxiliar – Cerena/IST-UTL

Doutor Martim Afonso Ferreira de Sousa Chichorro, Investigador. Auxiliar – FCT/UNL

Doutor José António de Almeida, Prof. Auxiliar – FCT/UNL

Doutor Paulo Alexandre Rodrigues Roque Legoinha, Prof. Auxiliar – FCT/UNL

FACULDADE DE CIÊNCIAS E TECNOLOGIA
UNIVERSIDADE NOVA DE LISBOA

June 2012

STOCHASTIC SIMULATION OF THE MORPHOLOGY OF FLUVIAL SAND CHANNELS RESERVOIRS

Acknowledgments

I am sincerely and heartily grateful to Doctor José António de Almeida and Doctor Paulo Legoinha for the idea to write this work, for possibility to work with them and also for guiding and correcting with attention and care throughout my thesis writing.

This master's thesis is supported by the Erasmus Mundus Action 2 Programme of the European Union.

Resumo

A caracterização de reservatórios de petróleo de tipo fluvial com algoritmos estocásticos constitui um problema complexo. Isto porque os canais apresentam padrões espaciais que não são caracterizados pelas estatísticas bi-ponto que estão na base dos modelos geoestatísticos. Entre estes aspectos contam-se, por exemplo, as morfologias deltaica, meandriforme e de planície aluvial, onde os canais formam um complexo padrão 3D resultante da acumulação de sedimentos pela antiga rede fluvial.

No presente trabalho apresenta-se uma metodologia inovadora destinada a gerar imagens da morfologia de canais arenosos em reservatórios fluviais, com base em um modelo de simulação 3D. É baseada nas seguintes etapas: (1) partir de histogramas do comprimento, largura e altura de canais de areia, e de um malha de pontos com orientações locais; (2) fazer a simulação estocástica das dimensões largura e altura de hipotéticos canais de areia (3) gerar e posicionar esqueletos de hipotéticos canais e associar as dimensões largura e altura geradas na etapa anterior (modelo booleano estocástico de tipo vectorial); (4) converter o modelo anterior para um modelo matricial, associando zonas com diferenciação da incerteza; (5) utilização do método de simulação de campos de probabilidade (probability field simulation – PFS) para pós-processar o modelo booleano na forma matricial obtido na etapa anterior. Os resultados do modelo são várias imagens equiprováveis binárias (canal / não canal) que podem posteriormente ser preenchidas por valores de porosidade e permeabilidade.

Esta metodologia foi testada com sucesso para a modelação de canais de areia de um reservatório fluvial do médio oriente. Concretamente, discutem-se os resultados do modelo obtido, faz-se uma análise do padrão de formas obtido na relação com a imagem de orientações locais de partida e tecem-se comentários sobre a incerteza local e global do modelo em função da conectividade dos canais.

Palavras-chave: reservatórios fluviais; canais de areia; geoestatística; modelos booleanos; modelos estocásticos.

Abstract

The characterization of fluvial-type oil reservoirs using stochastic simulation algorithms is a complex problem because the morphology of the channels are complex and are not fully characterized by the two-point statistics of the geostatistical models (variograms and/or spatial covariances). Among these features, for example, are delta morphologies and meander-form floodplain where the channels form a complex pattern of the resulting 3D sediment accumulation by the former waterway system.

This work presents an innovative methodology designed to simulate 3D stochastic images of the morphology of fluvial sand channels reservoirs. It is based on the following steps: (a) preparation of histograms of length, width and height of sand channels and a 2D image of local orientations; (2) simulate widths and heights of the hypothetical sand channels along their paths; (3) generate randomly skeletons of hypothetical channels and associate the width and height dimensions generated in the previous step (Boolean vector model); (4) convert the Boolean vector model into a raster model and link regions of uncertainty according distances to the skeleton; (5) finally, using the method of Probability Field Simulation (PFS) condition the Boolean model with a model of variogram and resolve the regions of uncertainty. The outputs are sets of binary images (channel – sand / not channel – shale) that can be filled by values of porosity and permeability.

This methodology was successfully tested for modeling channel sand reservoir of a river of the Middle East. Specifically, results are discussed in connection with the image of local orientations together with an analysis of the local and global uncertainties of the model.

Keywords: fluvial reservoirs; sand channels; geostatistics; Boolean models; stochastic models.

Contents

Figures

Tables

1. INTRODUCTION

The intensive and growing exploration of petroleum from reservoirs in the last decades, associated with a decrease of reserves, focus the interest in research and characterization steps which became more complex and expensive, raising the magnitude of risk decisions.

The main objective of the evaluation of petroleum reservoirs is forecasting production of oil and/or gas, including reserves assessment (potential oil in place) and the location of new wells. This involves modelling the fluid flow, which requires first modelling of petrophysical properties such as porosity and permeability. The petrophysical properties often differ between facies and therefore should be modelled separately for each facies, which means that modelling should be a two-step methodology, beginning with the morphology and followed by the properties simulated conditionally to the facies model. To this end, it is necessary a good model for the distribution of the reservoir facies (morphological model).

Fluvial reservoirs offer a particular challenge for modelling (Luis and Almeida, 1997) due to their variable geometries and complex networks. In particular fluvial sands reservoirs are characterized by their elongate shapes with a relatively small width-length ratio. In this regard, a very topical issue is the development of theoretical and methodological principles of using computer technology for resolving problems of prospecting and exploration of oil and gas for fluvial reservoirs.

Nowadays there are a lot of different approaches of modelling. There is no unique or 'best' approach that would be valid for all reservoirs of all types. In order to visualize reservoirs with complicated structures it is better to mix some of them. The choice of the "best" methodology always depends on geological, morphological and structural conditions, as well as data available.

Stochastic models of reservoirs are an important tool for assessing geological heterogeneity conditioned to different sources and detail of the available data, at all steps of reservoir development: discovery, evaluation of reserves, exploitation, enhanced recovery and closure. There are many techniques and methodologies for reservoirs modelling, but regarding the small amount of data they are typically simulation based (Deutsch and Journel, 1992; Almeida, 1999; Vargas-Guzmnan and Al-Qassab, 2006; Mata-Lima, 2008).

As it is known, oil and gas with commercial interest only exist in certain regions and under special conditions. Rocks in suitable stratigraphic positions, possessing porosity and permeability able to contain oil, or gas, or both in commercial quantities, are named reservoir rock. The most common types of reservoir rocks are clastic sediments (sandstones, conglomerates) and grained or crystalline carbonate rocks. This work deals with the particular class of clastic sediments, namely fluvial rocks.

The fluvial reservoirs represent about 20% of the world's remaining reserves of hydrocarbons, and are indeed an important reservoir type for the petroleum industry (Keogh et al, 2007). For a long time in petroleum reservoir description the modelled sedimentary deposits were represented as totally homogeneous bodies, both with regards to sedimentological and structural heterogeneities, in a gross simplification of their potential flow behaviour.

The aim of reservoir simulation models is to integrate data from multiple scales of measurement to capture a geologically realistic range and spatial variability in petrophysical properties, so as to be able to realistically simulate flow through them, as well as to be able to predict future oil and gas production of alternative recovery scenarios and to optimize field development.

The discovery of potentially large hydrocarbon accumulations within fluvial deposits in the Norwegian North Sea in the late 1970's to early 1980's, many fields in the Pennsylvanian Cherokee Group of Kansas, several fields in the Upper Pennsylvanian and Lower Permian on the eastern shelf of the midland Basin in West Texas, the upper part of the Sadlerochit formation at Prudhoe Bay in Alaska, the Upper Triassic sands in the Rankin gas fields on the northwest shelf of Australia, the approximately coeval sandstones in the Morecambe gas field of north-western England, all or most of the tar sands in the Uinta Basin of the USA (North, 1985) led to the realization that to produce these deposits economically and effectively, better prediction of their connectivity and flow behaviour requires the development of special modelling algorithms.

A wealth of sedimentary studies on outcrops and modern systems had already identified that fluvial deposits are heterogeneous on a variety of scales, from the microscopic to the megascopic scale (figure 1).

To better characterize these reservoir types and extract hydrocarbons it is important to understand the occurrence and variability of these various scales of heterogeneities. Also, predict heterogeneities caused by faulting are equally important in fluvial reservoirs characterization.

For modelling this type of reservoirs two approaches are currently used: Boolean and multi-point. In Boolean modelling channels are positioned in the volume under study in a deterministic or stochastic design of the skeleton of the channel. In the case of a deterministic positioning, one digitizes the position of the skeleton on 2 or 3D set (a range of arcs) based, for instance, on a seismic image. On the base of a skeleton is generated the channel's form after appropriation of a width and height throughout the skeleton. The multi-point approach starts from a theoretical or conceptual image of the shape of channels. From this image is extracted a multi-point statistic of elementary forms (templates) which are then reproduced by simulation in new images. From a theoretical standpoint the multi-point approach is effective but has two main problems that is why it is rarely used in practice: it requires a reference image and is computationally very difficult. The deterministic approach is thus preferable but in case of post-processed is unrealistic.

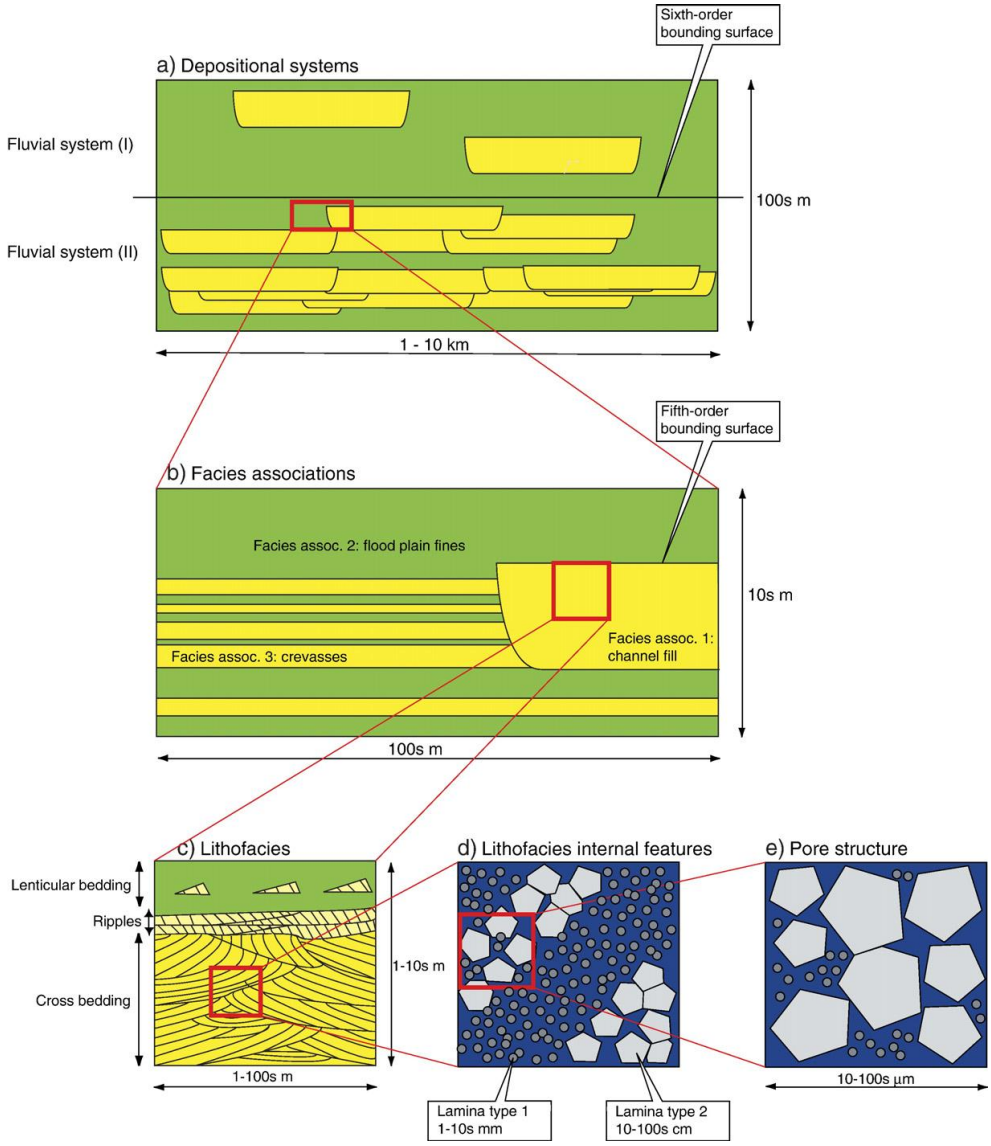

Figure 1 - Schematic view of the different scale and type of heterogeneities that can affect fluid flow behaviour in fluvial depositional systems (modified from Weber, 1986).

1.1 Organization of the thesis

This report is organized into six main sections. This first introduces the challenge of modelling fluvial sand channels. The second summarize the geological environments of these types of fields and the third presents some exploration methods and variables of interest. Section 4 describes the proposed methodology for simulation of fluvial sand channels and section five presents and discusses an example of channels modelling combining Boolean and stochastic algorithms. Finally, section 6 presents the final remarks.

2. GEOLOGICAL ENVIRONMENTS

2.1 Types of sedimentary rocks

To be able to create models of clastic reservoirs it is necessary to understand the geological environments of the reservoirs. There are two main groups of sedimentary rocks, which are classified on the basis of their origin:

- Chemical or biochemical;
- Clastic sedimentary rocks.

Also it can be mentioned another classification of sand deposits according to their environments:

- Terrestrial (Aeolian or dune sands);
- Tidal, deltaic, coastal;
- Deep marine and
- Fluvial (river deposits).

The most important types of sedimentary rocks in the production of hydrocarbons:

- Carbonates;
- Shales;
- Evaporites;
- Sandstones.

This work deals with the particular class of clastic sediments, namely fluvial rocks.

2.2 The main parameters of characterization of clastic rocks

The main characteristics of sedimentary particles can be described by determining their size, shape, sorting and composition. Size, shape and sorting define the texture.

2.2.1 The grain size

The grain size of the sediment is a function of many interrelated parameters, the most important of which are: proximity and composition of the source rock, weathering and transport processes and

physical energy distribution at the site of deposition (Fritz, 1988). The most common grain size classification is shown on the figure 2.2.1.

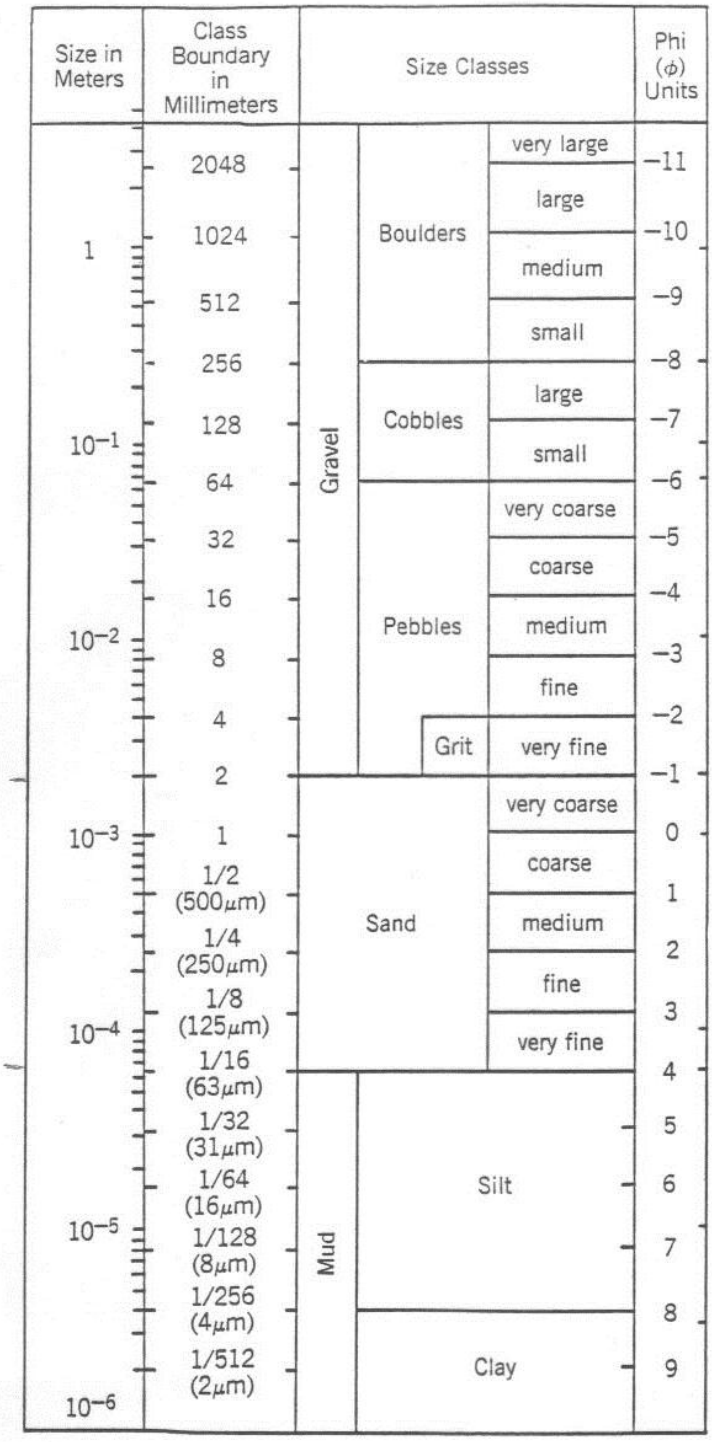

Figure 2.2.1 – Classification of sedimentary particles based on Wentworth's classification of grain size (Fritz, Moore, 1988).

2.2.2 **The grain shape, sphericity and roundness**

Because the shape of sedimentary grains in natural sediment can range it is essential to describe a shape variation as well. The most common method is a description of sphericity. Actually, the sphericity measures the equality of 3 mutually perpendicular axes through the grain, presented in Sneed and Folk's (1958) formula below: (L) – the length of the long, (I) – intermediate and (S) – short axes of the grain.

Maximum projection sphericity = $S^2 / (L\ I)$

These parameters are well represented by a Sneed and Folk's triangle (figure 2.2.2).

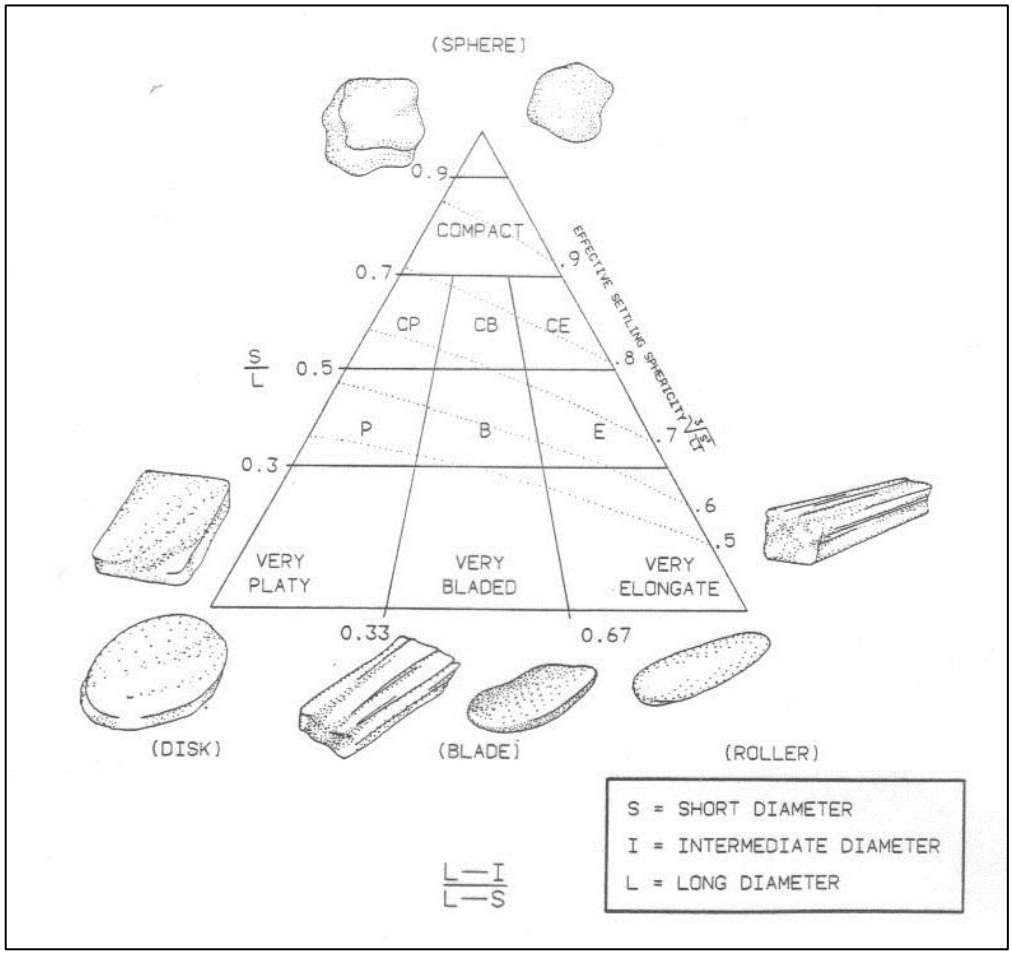

Figure 2.2.2 – Triangle diagram, illustrating the names given to various shapes of sedimentary particles, based on a method by Sneed and Folk (1958).

One more essential characteristic of sedimentary grains is calculated roundness. Its values range from 1.0 (perfectly rounded) to approaching 0.0 (very angular). In summary, roundness is a simple concept: an angular grain bristles with sharp corners and edges, a round displays relatively broad, smooth surface.

2.2.3 **Sorting of a sediment**

Sorting - is a measure of the dispersion of the grain-size distribution of sediment. Because it is very difficult to determine the grain-size distribution of sediments rapidly, without detailed thin-section analysis, most sorting determinations are made by comparison to a standard drawing.

Because it would be very effortful to measure sand-sized grains, small 25-75 g samples are analyzed by sieving in a nest of sieves with various mesh sizes with a shaking nest machine for a specified period of time. Because grains of different shapes may all have an equivalent sieve diameter (figure2.2.3), sieve analysis is generally assumed to measure intermediate (I or b) axis of the grain. Sorting influences porosity (subchapter 2.2.4).

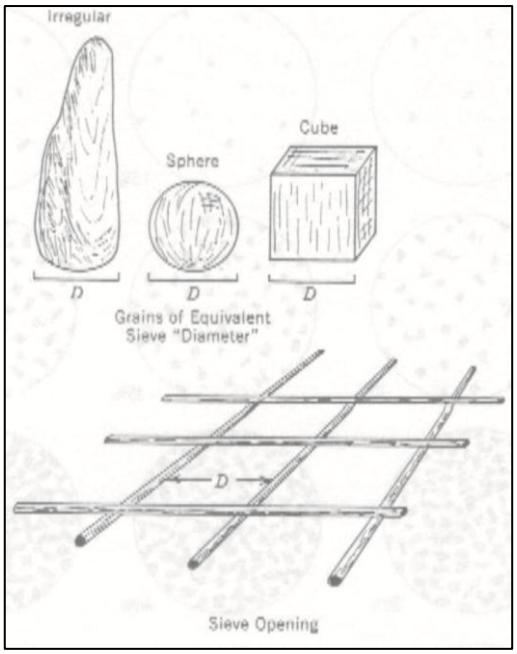

Figure 2.2.3 – Diagram illustrating the equivalent sieve diameter of different shaped grains (Fritz, Moore, 1988).

For that matter sorting and grain size present some relation with specific types of environments (figure 2.2.4).

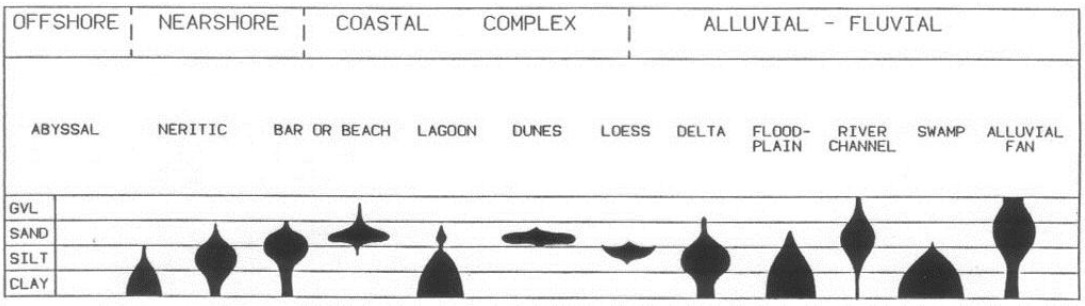

Figure 2.2.4 – Sorting and grain size distribution for sediments from a variety of environments (Folk, 1974).

2.2.4 **Porosity and permeability**

Porosity is the ratio of void space in a rock to the total volume of rock, and reflects the fluid storage capacity of the reservoir. Distinguish following types of porosity:

- Primary Porosity— an amount of pore space presents in the sediment at the time of deposition, or formed during sedimentation. It is usually a function of the amount of space between rock-forming grains;
- Secondary Porosity— a post depositional porosity. Such porosity results from groundwater dissolution, recrystallization and fracturing;
- Effective Porosity versus Total Porosity— an effective porosity is the interconnected pore volume available to free fluids. Total porosity is all void space in a rock and matrix whether effective or noneffective (figure 2.5);
- Fracture porosity – a results from the presence of openings produced by the breaking or shattering of a rock;

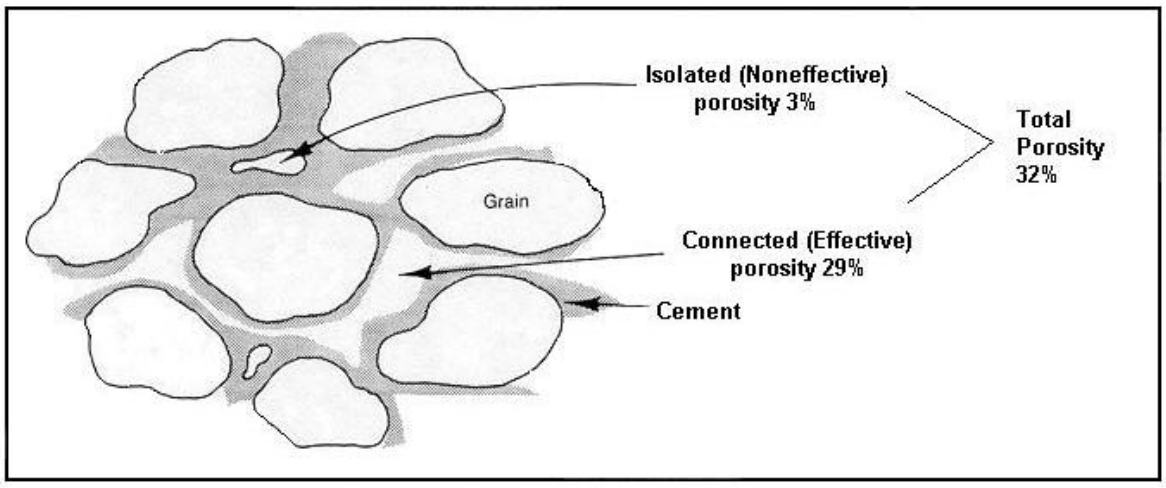

Figure 2.5 – An example of some type of porosity (Basic Petroleum Geology and Log Analysis, 2001).

Porosity can approach, in very well sorted sand, a theoretical maximum of 47.6%. In sandstone, this value is typically much lower due to cementation and compaction. Also porosity is generally higher in well than in poorly sorted rocks (Basic Petroleum Geology and Log Analysis, 2001).

Likewise a formation must have interconnected porosity in order to be permeable. Permeability is a measure of the ease with which a formation permits a fluid to flow through it. Porosity and permeability have specific relations. There are some examples of variations in permeability and porosity:

- Some fine-grained sandstones can have large amounts of interconnected porosity; however, the individual pores may be quite small. As a result, the pore throats connecting

individual pores may be quite restricted and tortuous; therefore, the permeabilities of such fine-grained formations may be quite low;

- Shales and clays which contain very fine-grained particles often exhibit very high porosities. However, because the pores and pore throats within these formations are so small, most shales and clays exhibit virtually no permeability.

2.2.5 **Textural maturity**

Grain size, sorting, rounding and shape have been used to determine the textural maturity of sediment. Sediments, deposited very close to their source with short distance or time of transport, are texturally immature whereas those that have been transported long distance over long periods of time become texturally mature. Texturally immature sediments are characterized by poor sorting with angular grains; they contain much clay and many non-spherical grains. By its turn, texturally mature have well-rounded grains of all the same size; contain no clay and may have many spherical grains.

2.2.6 **Composition**

To accurately describe a sedimentary rock, it is necessary to define its composition. Grains that form sedimentary rocks can be divided into detrital and non-detrital categories. Detrital particles are those derived from erosion of source area (pre-existing rock) transported and then deposited. Non-detrital grains initiate from organic and/or inorganic processes within the basin of deposition. Also whether detrital or non-detrital all compositional elements should be estimated by percentage (figure 2.2.5).

All of these characteristics – size, sorting, shape and composition – are essential in understanding the origin of sedimentary particles and the history of the sedimentary rock.

2.3 Types of sandstones and geological setting

Sandstone classification is represented by three principal types according to initial composition:

- High-quartz sands (totally dominated by detrital quartz);
- Feldspathic or arkosic sandstones (contain significant quantities of unweathered feldspar);
- Litharenites (with high contents of lithic fragments or clay matrix).

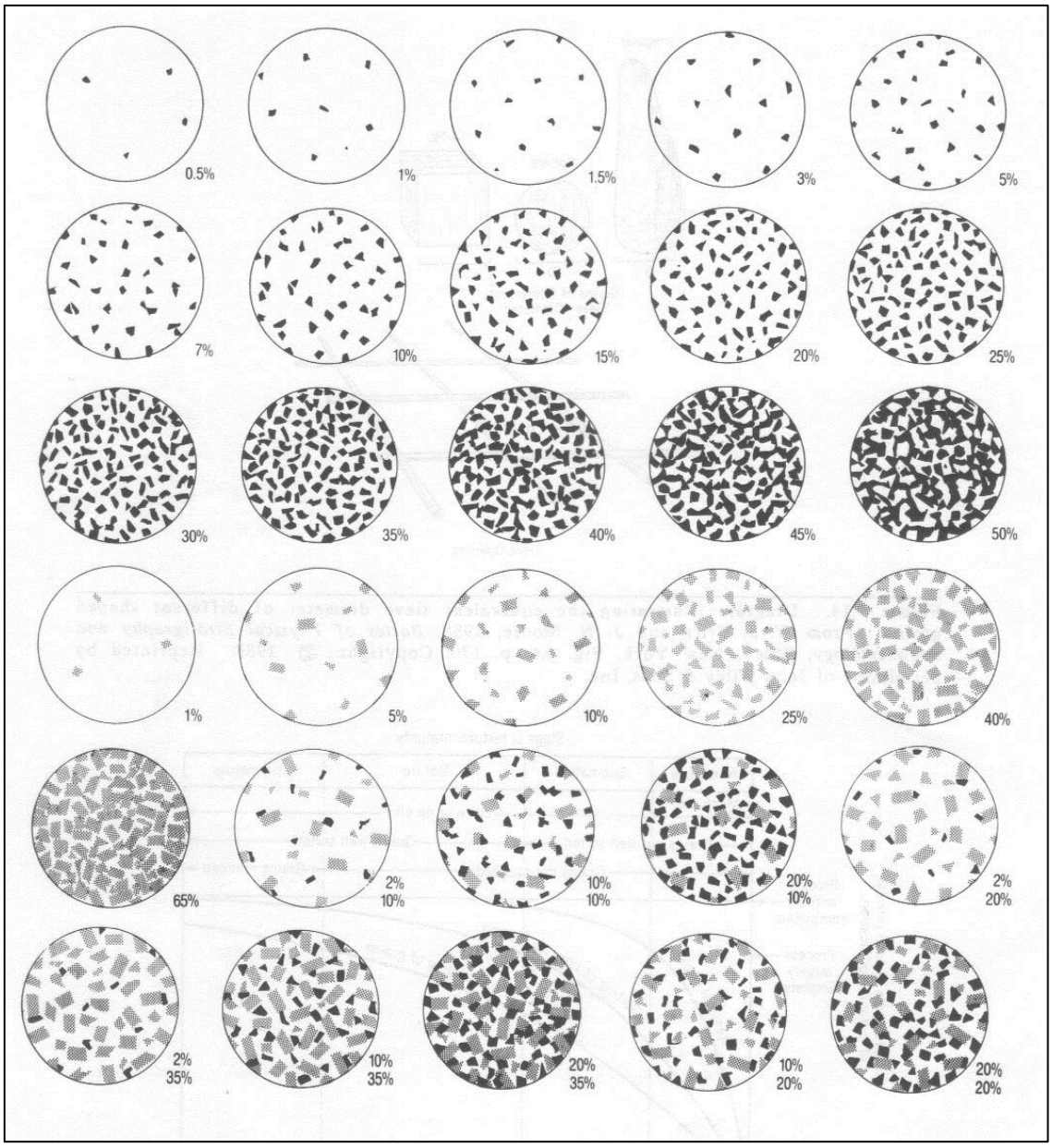

Figure 2.2.5 – Figure for estimating percentage of a component by volume (Compton, 1985).

The main interest to geologist is high-quartz sand. High-quartz sands sediments are provided by three widespread continental terrains and geological settings:

- Much thicker bodies of high-quartz sandstone comprise the molasses shed into foreland or backarc basins from newly risen fold-trust belts (the eastern Caucasus).
- In low relief cratonic interiors with sands derived from the basement or from older sedimentary sources (Illinois Basin, the Mississippi);
- In tectonically quiescent continental margins of the Atlantic type (the Niger delta);

The most part of high-quartz sands are referred to rivers.

2.4 Types of the rivers and their characteristics

River channels in sedimentary basins vary greatly in size. The magnitude of any channel may be described in terms of its width and depth (height). This basic measurements help to determine the extent of coarse-grained channel deposits. Also the mean annual discharge is very significant for channel characterization.

As river channels possess form and magnitude it is possible to describe them (figure 2.4.1) by combination of:

1) a planform description of channel deviation from a straight path (sinuosity, P);
2) the degree of channel subdivision by large migrating bedforms and accreting islands around which channel reaches diverge and converge (braiding);
3) more permanent distributive channel subdivision into stationary smaller channels (separated by floodplain) that each contain their own channel and point bar (anastomosing).

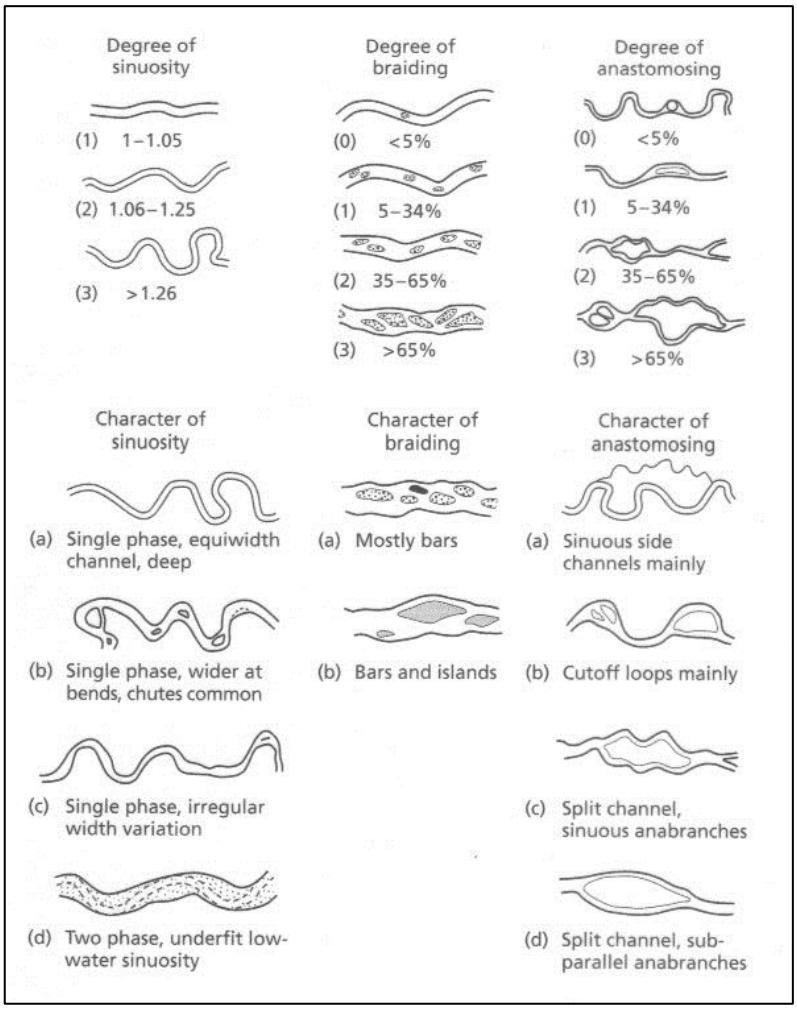

4) Figure 2.4.1 – Sketches to show the range of river channel types (adapted after Brice, 1984).

The first and the second may be expressed as numerical indices, but commonly it is more appropriate to use qualitative terms, for instance, highly sinuous, moderately braided, etc.

According to this occurs following types of rivers (figure 2.4.2).

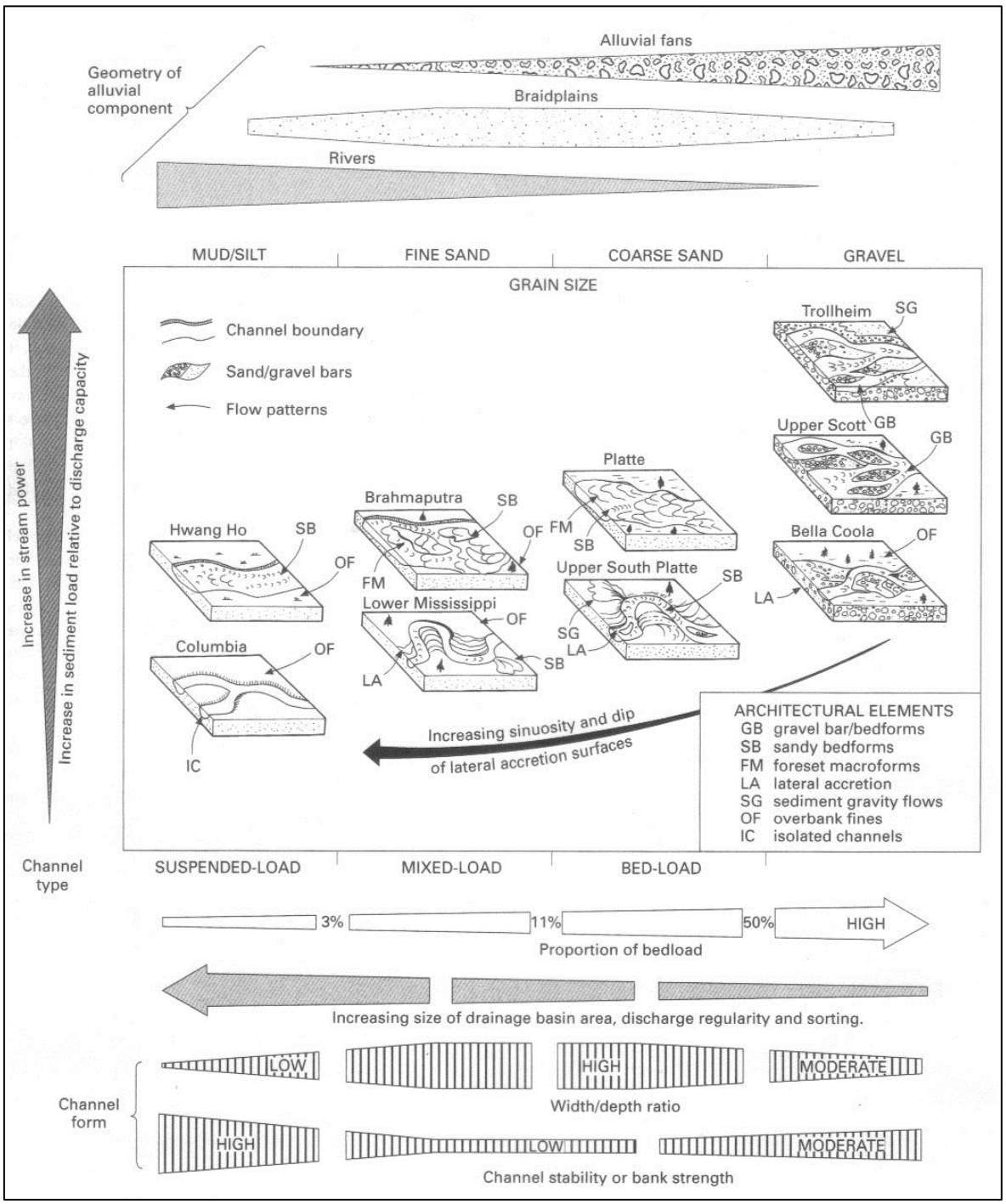

Figure 2.4.2 – Channel types related to the dominant type of bedload in the stream and the relative stability of channel banks (after Orton & Reading, 1993).

2.4.1 **Braided rivers**

Rivers of this type consists of several or many branching, unstable channels of low sinuosity are characterized by abundant coarse bedload, forming bars, islands, and channel-floor deposits (figure 2.4.3a).

The channel complex typically occupies most of the valley floor, leaving little room for a floodplain. Glacial outwash streams and ephemeral streams draining mountainous areas in arid regions are normally braided, and may form broad sheets of sand or gravel crossed by networks of shallow, shifting channels.

a)

b)

c)

d)

Figure 2.4.3 – a) Braided river, Denali National Park, Alaska (Walsh, 2007); b) meandering river, Williams river, Alaska (Smith, 2007); c) anastamosed river, avulsion belt of the Saskatchewan River (Smith, 2007); d) straight river, Kaa-Khem River, Siberia, Russia (Reuters, 2008).

2.4.2 **Meandering rivers**

These are single-channel streams of high sinuosity, in which islands and midchannel bars are rare (figure 2.4.3b). Sediment in these rivers ranges from very coarse to very fine. A significant

proportion of the bedload typically is deposited on the insides of meander bends, forming point bars. The channel, with its coarse deposits, may be confined to a narrow belt within an alluvial valley, flanked by a broad floodplain, upon which deposition of fine-grained sediment takes place only during flood events, seasonally or at longer intervals.

2.4.3 **Anastomosed rivers**

These develop in stable, low-energy environments or in areas undergoing rapid aggradation. They consist of a network of relatively stable, low- to high-sinuosity channels bounded by well-developed floodplains. Channels are characteristically narrow and accumulate narrow, ribbon like sandstone bodies (figure 2.4.3c).

2.4.4 **Straight channels**

These are rare, occurring mainly as distributaries in some deltas (figure 2.4.3d).

Rivers which emerge from a mountainous catchment area into a low plain drop their sediment load rapidly. The channel may bifurcate, becoming braided in character. The typical results are a distinctive landform and an alluvial fan (see subchapter 2.9.2).

2.5 Types of river deposits

Some quantities of fluvial sands depend on the parts of the river where they are deposited. The main parts of the river system in which significant sand bodies are deposited and preserved are the braided section (with many channels) and the meander belt (with a single master channel on a wide floodplain). It is possible to mark out feature appearances of deposits depending on location. For example, a braided stream deposits are longitudinal and transverse bars of sand. In an upper low amplitude meander belt are developed point bars on the insides of curves; in a lower meander belt – multiple point bars. Sometimes the fluvial deposits may merge into the more widespread delta plain deposits which include distributary channel sands.

Thereby river deposits of sediment occur as four main types:

1. **Channel-floor sediments** consist of the coarsest bed load, such as gravel, waterlogged vegetation, or fragments of caved bank material;
2. **Bar sediments** are accumulations of gravel, sand, or silt which occur along river banks and are deposited within channels, forming bars that may be of temporary

duration, or may last for many years, eventually becoming vegetated and semipermanent (figure 2.5.2);

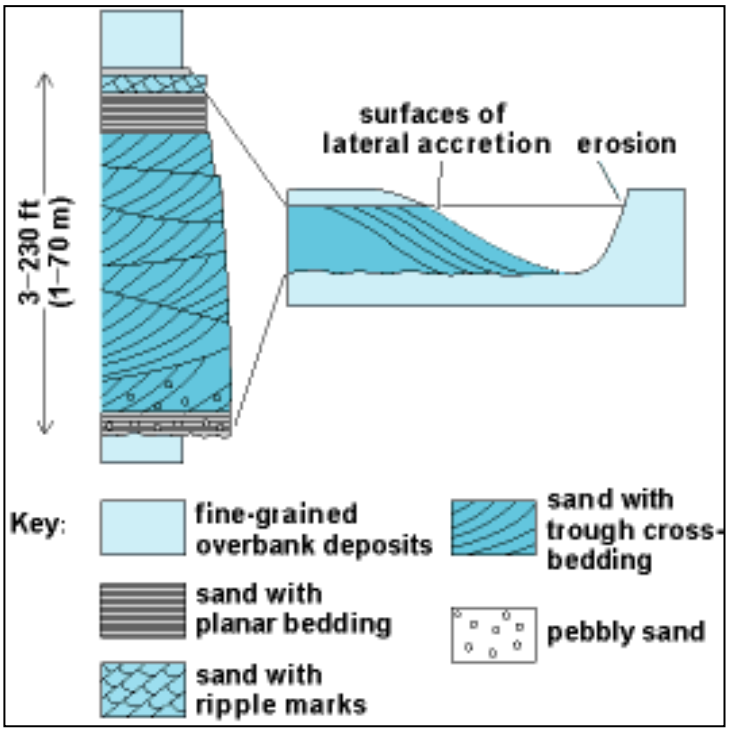

Figure 2.5.2 - Development of a fining-upward succession by lateral accretion of a point bar, (Miall, 2008).

3. **Channel-top** and **bar-top** sediments are typically composed of fine-grained sand and silt, and are formed in the shallow-water regions on top of bars, in the shallows at the edges of channels, and in abandoned channels;
4. **Floodplain deposits** are formed when the water level rises above the confines of the channel and overflows the banks. Much of the coarser floodplain sediment is deposited close to the channel, in the form of levees; silt and mud may be carried considerable distances from the channel, forming blanket like deposits.

2.6 Facies associations and sedimentary cycles

Depending on the nature of the sediment load of the river, fluvial sediments may be dominantly conglomeratic, sandy, or silty. This characteristic described by a function of slope and the proximity to sources, but also by a reflection of sediment availability. Likewise they depend on climate, for instance, humid climates favour chemical and biochemical weathering processes, which yield a large suspended or dissolved sediment load; coarse detritus is more typically the

product of drier climates, in which mechanical weathering processes (such as frost shattering) are dominant.

It is possible to observe some vertical spatial order in the sedimentary facies described above: from channel floor to floodplain. This order is based on decreasing grain size upward. Such deposits may be composed by a series of fining-upward successions, or cycles, each a few meters to few tens of meters in thickness (figure 2.6.1).

There are a variety of causes of such cycles. The first that was recognized is the mechanism of lateral accretion, whereby point bars enlarge themselves in a horizontal direction as the meander bounding them migrates by undercutting the bank on the outside of the bend. The depositional surface of the point bar may be preserved as a form of large-scale, low-angle cross-bedding within the deposit, its amplitude corresponding approximately to the depth of the channel. Similar cycles may be caused by the nucleation and growth of large compound bars or sand flats within braided channel systems. The accretion surfaces, in such cases, may dip in across- or down-channel directions. Individual flood events, especially on the sand flats of ephemeral stream systems, may form sheetlike flood cycle deposits up to a meter or so thick, the upward fining corresponding to decreasing energy levels as the flood waned. The gradual choking of a channel with sediment, and the progressive abandonment of the channel, will also generate a fining-upward cycle.

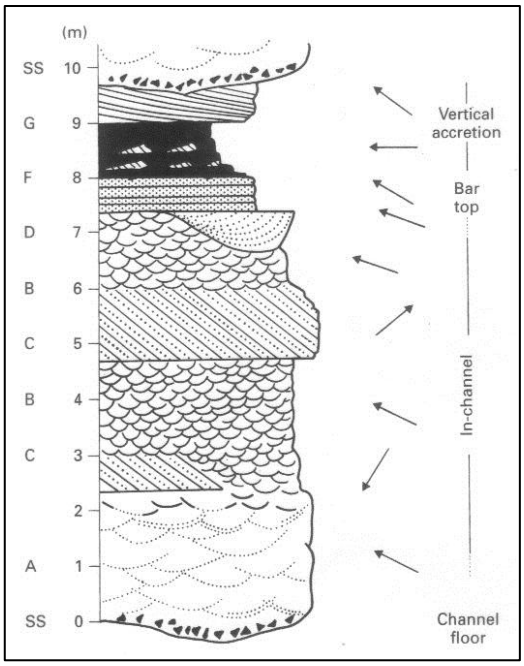

Figure 2.6.1 – Facies model for the Battery Point Sandstone based on analysis of vertical facies transitions through many channel units. The model presents an ideal that is seldom complete in nature (after Cant & Walker, 1976).

2.7 Tectonic Setting of Fluvial Reservoirs

The thickest and most widespread fluvial deposits accumulate in a few specific tectonic settings. This group is divided into two main categories – extensional basins, and basins associated with plate collision. Petroleum in fluvial mostly occurs in rift basins and foreland basins. This localization of petroleum can be explained by specific types of tectonic setting where fluvial deposits are volumetrically important to constitute a distinctive category of reservoir body. Such producing units are divided into several types concerning the tectonic setting:

- Backarc foreland basins (Cano Limon oil field of Colombia);
- Backarc basins (Daqing field, China);
- Forearc basin (Cook Inlet, Alaska);
- Collision-Related Basins (Ordos Basin, China);
- Basins in Continental-Transform Setting (the South Belridge field, California);
- Rift basins (Gippsland Basin, Australia);
- Basins on External Continental Margins (The Gulf Coast of the United States);
- Intracratonic basins (Cooper Basin, Australia);

2.8 Styles of Fluvial Reservoir

The stratigraphic criteria can define three major types of nonmarine reservoirs, as shown in table 2.8 and figure 2.8.1

The primary criterion used in this classification is the type of depositional system – clastic wedge versus incised paleovalley. The second criterion is reservoir geometry. Incised-valley fills are ribbon bodies, clastic wedges consist of either sheet bodies or multiple lenses and ribbons enclosed in impermeable fine-grained sediment. Last column presents most typical tectonic setting.

Table 2.8 – The three major types of petroleum reservoir in fluvial sandstones (Miall, 1996)

Type	Code	Depositional system	Reservoir geometry	Most typical tectonic setting
Paleovalley	PV	Incised valley	Ribbon	Foreland basin
Sheet	SH	Clastic wedge	Sheet	Rift basin, extensional margin
Channel and bar	CB	Clastic wedge	Multiple lenses, ribbons	Foreland basin, extensional margin

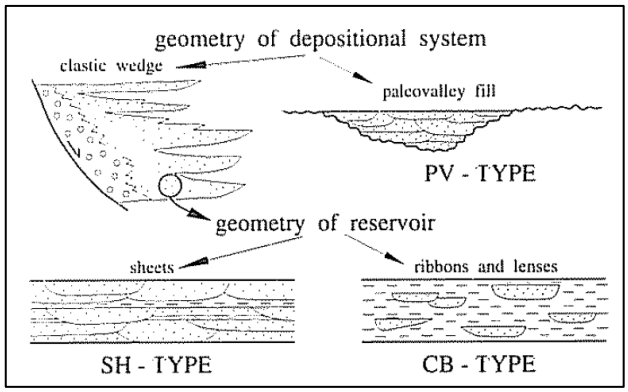

Figure 2.8.1 – Classification of nonmarine reservoirs according to the geometry of the depositional system and the geometry of the reservoir body (Miall, 1996)

2.8.1 **Paleovalley Bodies (PV Type)**

Paleovalley bodies are distinguished by the ribbon or shoestring shape of the reservoir and by their association with regional unconformities. The reservoirs typically tens of kilometers in length, up to a few kilometers in width, and several tens of meters in thickness. The fill may be entirely fluvial, or it may contain an estuarine component (Wood and Hopkins, 1992).

PV-type fields can occur only paleovalley fill is incised into impermeable strata, and also a top seal and a structural component are necessary for them to generate a trap. Another type of trap is related with the paleovalley that is folded over an anticline.

Good examples of PV-type fields are South Ceres field, Oklahoma (Lyons and Dobrin, 1972), Recluse field, in Powder River Basin (Woncik, 1972), and Midland field, Kentucky (Reynolds and Vincent, 1972).

2.8.2 **Sheet Bodies (SH Type)**

Sheet sandstones reflect high source-area relief and steep paleoslopes, with a development in most cases of a broad braidplain. Most fields of this type require a structural trapping mechanism, because the reservoir consists of a sheetlike porous unit providing little of fluid or not providing it at all. Most of such type's cases consist of large faulted anticlines in which the reservoir sandstone is overlain by impermeable shale, for example, the Hassi Messaoud field of Algeria. Techniques of surveillance geology (pressure tests and fluid-flow monitoring) are very powerful tools for subsurface mapping for these type reservoirs (Miall, 1996).

SH-type reservoirs appear with fairly uniform internal heterogeneity within reservoir bodies at an early exploration stage (for instance, Prudhoe Bay, Alaska), but latter they may be considered as CB type.

2.8.3 Channel-and-Bar Bodies (CB Type)

CB-type fields are characterized by the small size of individual reservoir body, even in some cases there may be hundreds to thousands of individual reservoirs units, can add up to significant accumulations. Development of these fields may be extremely difficult, because they consist of the "labyrinth" and "jigsaw" types of reservoirs (Weber and Van Genus, 1990), with tortuous flow paths. Typical traps are entirely stratigraphic. Good examples of CB-type fields are Citronelle field, Texas (Eaves, 1976), and Daqing field, China (Yinan et al., 1987).

Prospecting, definition of traps and development of production models for this field type, require a detailed knowledge of depositional style. Seismic-stratigraphic mapping is important in the delineation of small structural-stratigraphic traps, especially for basins, which are entering the mature exploration phase, for instance, Cooper basin in Australia (Elliott, 1989).

An important aspect for production modeling may be to ascertain the degree of interconnectedness of the reservoir units, and the definition of separate flow units within the field.

2.9 Alluvial sediments

Sometimes fluvial deposits are a part of another type – alluvial fans, extending from the subaerial regime to the submarine. A river is continually picking up and dropping solid particles of rock and soil from its bed throughout its length. Where the river flow is fast, more particles are picked up than dropped. Where the river flow is slow, more particles are dropped than picked up. Areas where more particles are dropped are called alluvial or flood plains and the dropped particles are called alluvium.

Even small streams make alluvial deposits, but it is in the flood plains and deltas of large rivers that large, geologically-significant alluvial deposits are found.

2.9.1 Alluvial processes

Alluvial morphologies and deposits are products of complex interactions of erosion and deposition with the balance between them varying between different settings (Reading, 1996). Erosion occurs at a range of physical and temporal scales. At the smallest scale, floods erode loose sediments and

cut small scours in cohesive fine sediment. At the large scale, floods cut new channels that range in size from channel belts to overbank channels. Once channels are initiated, they may expand and shift position through a combination of vertical inclination (the vertical cutting of the substrate so that the channel deepens) and lateral migration (associated with lateral erosion). Moreover, the transport and depositional processes that occur in alluvial channel (debris flows, bedload, suspended load and wind) influence on sorting (for instance, fine grained, poorly sorted) and bedforms deformations (for instance, ripples, dunes, plane beds). When sediments deposited on alluvial fans, floodplains and in river channels they become susceptible to alteration, which cause different physical modifications. Texture and mineralogy are modified by soil-forming processes and early digenesis.

Thus, knowing the relationship between processes and characteristic features of the rocks it is possible to determine the conditions under which sediments were deposited, or, studying the conditions helps to predict the type of potential sediments.

2.9.2 **Alluvial fans**

Alluvial fans are a form of fluvial depositional system distinguished on the basis of geomorphic character rather than by a characteristic fluvial style.

Alluvial fans are localized areas of enhanced sedimentation downstream of points where laterally confined flows expand. Confinement is usually within a narrow valley or gorge cut into an area of high relief. Flow expansion causes a reduction in depth and velocity which leads to deposition. Alluvial fans vary enormously in scale and in terms of their active processes. Both of these reflect a combination of source area lithology, catchment size and climate.

3. PROSPECTION METHODS AND INTEREST VARIABLES

To construct the model of reservoir is easier when parameters can be obtained by direct measurements. Concerning the channel parameters it is extremely difficult because the reservoir is located several thousands of meters underground and can only be described through indirect measurements. Also they are difficult to map in detail because of frequency of lateral facies changes and the lack of distinctiveness of individual beds in successions consisting of repeated similar channel and overbank units (Miall, 1996). Estimating channel parameters from indirect measurements is difficult for the following reasons:

1. Channels have irregular geometric shapes;
2. The spatial distributions of channels can only be known at very few locations (wells);
3. Permeability and porosity are spatially dependent;
4. Information is scarce;
5. Measurement techniques possess limited accuracy;
6. Data are obtained with errors;
7. The construction of mathematical models is usually not exact and complete;
8. The response of a reservoir is complex and must be computed making use of a numerical simulator.

Nevertheless there are plenty of methods of collecting data.

3.1 The use of marker bed

The usefulness of channels deposits for mapping purpose is limited because they are not laterally extensive. However, a few types of fluvial facies may be extensive enough to be useful for regional mapping purpose. In addition, nonmarine environments are the ideal location for the preservation of tephras, and these may extend for tens or hundreds of kilometres, providing ideal marker horizons.

3.2 Wireline Logs

This technic is very old, but it is very useful for correlation purposes and helps in interpreting fluvial style. Gamma ray logs record the presence of natural radioactivity, which typically is highest in clay minerals (typical seals). However, the presence of clay-rich clasts in clean, coarse sandstone may distort the reading, and feldspar-rich sandstones also yield high gamma-ray reading

(high potassium content). Thereby the most effective use of logs is in conjunction with other lithofacies mapping techniques.

3.3 Lithofacies Mapping

These techniques as mapping of net send content, or sand/shale ratio, or net pay are standard procedures for the delineation of reservoirs and for use in subsurface trend prediction. However, these techniques are limited in usefulness for exploration in fluvial environments, because of the significant facies variations, the thinness of the sandstone bodies, and their lack of directional predictability. Narrow channels and small point bars may be missed, because in most exploration situations well spacing is considerably bigger than the average dimensions of the typical sandstone body. However, where well density is sufficient, detailed lithostratigraphic subdivision and channel mapping may be rather effective.

3.4 Seismic Methods

Fluvial sandstones are commonly characterised by lenticular sandstone bodies, including paleovalleys, cannels, and bars, but these may be difficult to detect on reflection-seismic records, because of their small size and poor acoustic contrasts between the sandstone body and its host strata (Miall, 1996). Sandstone channels can be identified and mapped using seismic data, but the best results conduce to be achieved only when enough amount of local information is available, for instance by stratigraphy reading. In other words, seismic data should not be used as the only prospecting tool for fluvial sand bodies in frontier areas, but they may prove invaluable for extending fields or finding infill fields in well-known areas. For instance, paleovalleys may yield good reflections, as may a sandstone that is porous and gas filled.

The use of 3-D seismic method showed great results in detailed mapping of channels and bar deposits in PV- and CB-type field, and even in definition of reservoir heterogeneity in SH-type fields (figure 3.4.1).

3.5 Ground-Penetrating Radar

Ground-penetrating radar (GPR) uses radar pulses to image the subsurface; method uses electromagnetic radiation in the microwave band (UHF/VHF frequencies) of the radio spectrum, and detects the reflected signals from subsurface structures. Reflections occur at the interface of

beds with contrasting electrical properties, and the depth of penetration depends on the attenuation of the signal. Greatest penetration and lowest reflectivity are yield by unconsolidated sands, gravels and dry sandstones.

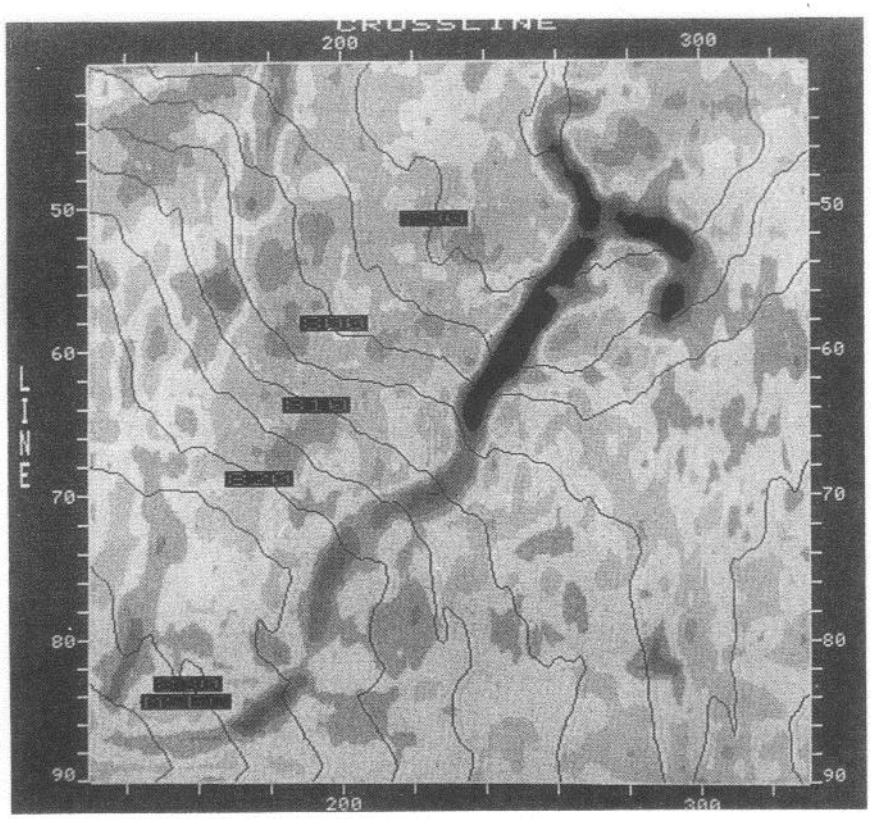

Figure 3.4.1 – Horizontal slice section, part of 3-D seismic section showing bifurcating deltaic distributaries, Cenozoic, Gulf of Mexico (Brown, 1991).

Several applications have demonstrated the ability of the tool to map architectural details in fluvial deposits up to 30 m in depth and 10 cm resolution. The main application of the technique is the evaluation of sand-body architecture to study the reservoir heterogeneity.

3.6 Magnetostratigraphy

Magnetostratigraphy is used to date sedimentary and volcanic sequences. The method works by collecting oriented samples at measured intervals throughout the section (figure 3.6.1). The samples are analysed to determine their characteristic remanent magnetization (the polarity of Earth's magnetic field at the time a stratum was deposited). This is possible because volcanic flows acquire a thermoremanent magnetization and sediments acquire a depositional remanent magnetization, both of which reflect the direction of the Earth's field at the time of formation.

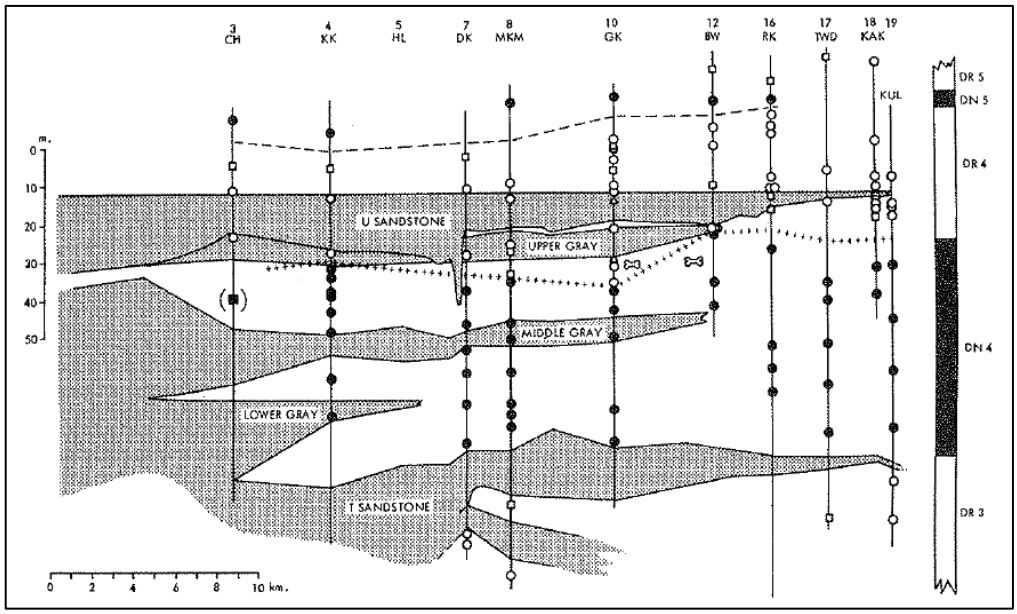

Figure 3.6.1 – Magnetic sampling of fluvial succession, the Miocene-Pliocene Siwalik Group of Pakistan. Black sample points, normal polarity, open points, reserved polarity (Behrensmeyer and Tauxe, 1982).

Not all fluvial deposits are good for paleomagnetic study. The quality of the results decreases hardly with increasing age, because of diagenetic complications, and reliable results depend on the presence of fine-grained facies (because the best magnetic signature is obtained from such units) at least every few meters from the succession.

3.7 Paleocurrent Analysis

Paleocurrent analysis is used to provide the following information:

1) Changes in channel and bar orientation and directional variability through a stratigraphic unit (as an indicator of vertical or lateral changes in fluvial style);
2) Vertical changes in flow direction through a stratigraphic section as indicators of interacting fluvial systems, or vertical changes in orientation of a system (as a response to paleogeographic changes).

The use of paleocurrent data to reconstruct the details of a fluvial depositional system is a well-established practice. Integrated basin-analysis methods couple paleocurrent data with data on facies and grain-size trends, and perhaps information on detrital sediment composition and possible sediment sources, the combination providing a powerful mapping technique (Miall, 1996).

3.8 The Dipmeter

The use of dipmeter as a tool for the detection and mapping of sedimentary dips promotes by logging companies, such as Schlumberger. There are 3 main applications in the study of fluvial sandstones:

1) The mapping of dipping fourth- and fifth-order surfaces corresponding to bar-top and channel-floor surfaces, and the drape associated with them, providing information on the shape and orientation of these features;
2) The mapping of internal, second- and third-order erosion surfaces (figure 3.8.1), that would facilitate the mapping of macroforms (such as point bar);
3) The mapping of cross-bed orientations for the paleocurrent information they yield.

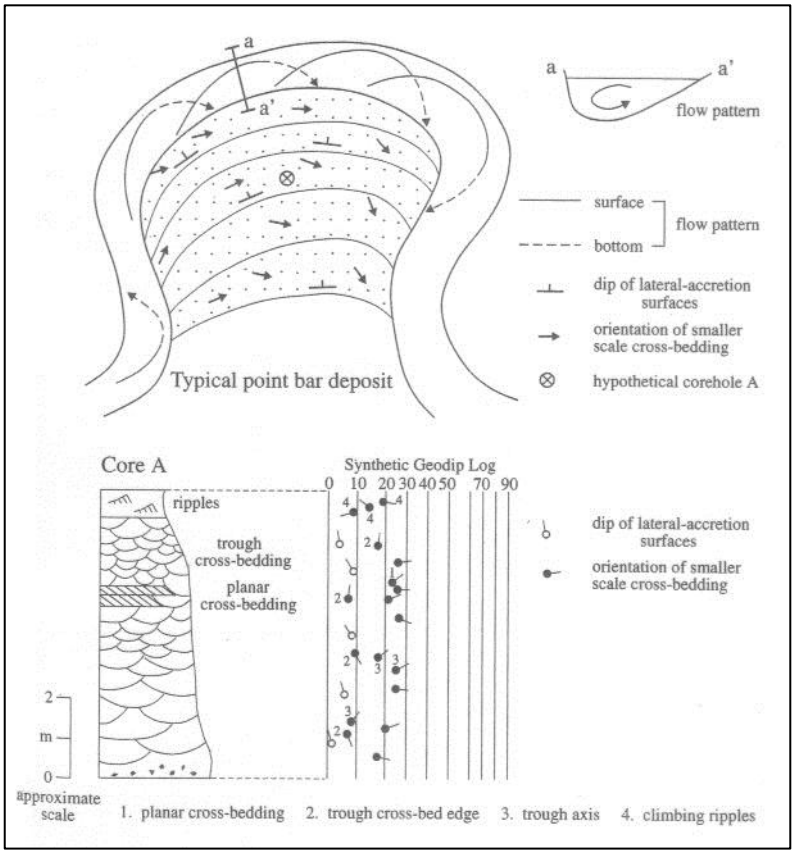

Figure 3.8.1 – Typical point bar and the dipping surface associated with it. The speculative dipmeter log is also shown (Miall, 1996).

However, there are many complications for application of this technique in fluvial deposits: the scale of cross-bedding approaches the limit of resolution at a few tens of centimetres or less and there are many types of surface that can produce confusion (for instance, contain reactivation surfaces).

3.9 Surveillance Geology

Surveillance geology is the monitoring of pressure and fluid composition of producing wells. Pressure data can be used to determine the connectedness of specific sandstone bodies, and fluid composition can be used to track the movements of oil front. Pressure-depth plots can be used to test reservoir body connectedness (Lorenz, 1991). This information, in addition, provides data to refine the depositional model (figure 3.9.1).

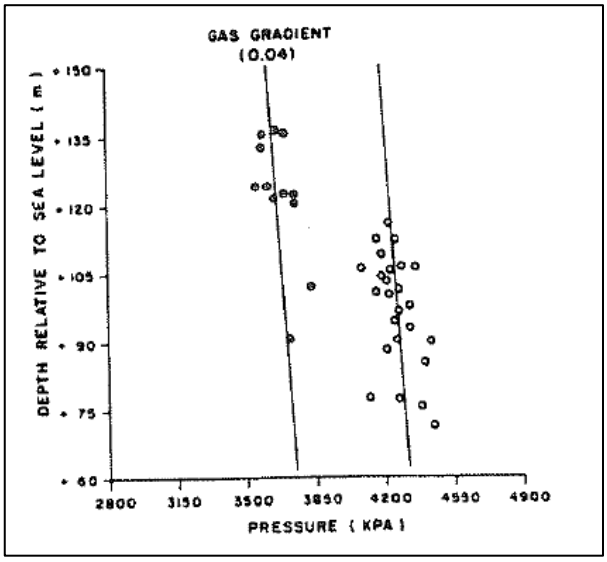

Figure 3.9.1 – Use of pressure-depth plot to test lithographic correlation. The points fall into 2 groups, indicating that they represent 2 channel-fill sandstone bodies isolated from each other by fine-grained units. Mannville Sandstone, Alberta (Putnam and Oliver, 1980).

The pattern of the flow of oil and water depends on the porosity-permeability architecture of the reservoir, and careful attention to the fluid movements can lead to continual refinements in the architectural model of the reservoir.

Information on reservoir architecture and fluid movement patterns is used in production simulation models.

3.10 Types of data and their applications

Data of different nature are collected during the life of a reservoir and can be grouped into two classes as static and dynamic data. Static data is time-independent and has no association with fluid transport. Geological, geophysical, petrophysical, seismic and geostatistical information are classified as static data. Dynamic data comprise those related to the transport of fluid and are time-

dependent. This type of data could be derived from pressure transient test, shut-in surveys, down hole permanent gauges, production history, water-cut, gas-oil ratio (GOR), and 4-D seismic surveys.

Inverting both static and dynamic data simultaneously for reservoir characterization is a difficult problem. A common procedure in practice is to upscale a fine-scale geological/geostatistical model generated conditioning to static data. The upscaled model is then adjusted in such a way to quantify dynamic data observed in the field. Current techniques for this adjustment are disconnected from the procedure of generating the original fine-scale model. Consequently, the final reservoir model constructed may honor the dynamic data but may not honor static data and in many cases, is unacceptable from a geological point of view.

For reservoirs characterized by simple configurations, the model obtained by these methods provides a good reservoir description and is sufficiently reliable for use in predicting future reservoir performance. However, other cases, particularly in many fluvial systems, often require a more reliable model - the model that honors the most available information. The introduction of dynamic data (time-dependent data) in the problem of characterization of fluvial reservoirs is useful in terms of obtaining detailed model configurations and significantly reducing the uncertainty in modeling and in reservoir predictions.

4. METHODOLOGY AND THEORETICAL BACKGROUND

Fluvial reservoirs offer a particular challenge for modelling (Matheron et al, 1987; Luis and Almeida, 1997) due to their variable geometries and complex networks. In particular fluvial sands reservoirs are characterized by their elongate shapes with a relatively small width-length ratio.

For modelling this type of reservoirs are currently often used following approaches: object or Boolean models, multi-point models and Sequential Indicator Simulation (table 4). Object models create realistic representations of the reality based on simple geometrical figures. They are often used to model geological structures where the geometry is the most important characteristic and the shape of the objects is not cellular or raster based. Some of the most common examples are faults, fractures and detritic channels (Deutsch and Wang, 1996; Holden et al, 1998; Almeida and Barbosa, 2008). Object models of fractures and faults approximates these objects as simple polygons (squares, circles, rectangles), whereas channels are presented by skeletons and polygons. Multi-point geostatistical models became recently often used, but they required training images to compute multi-point statistics, which are not always available (Strebelle, 2002; Hu and Chugunova, 2008; Peredo and Ortiz, 2011). Also they are computationally intensive and for both reasons they stay nowadays in a research state of the art.

Table 4 – Comparison of modelling approaches

Data characteristics	Sequential Indicator Simulation	Object Model	Multi-point statistics	Object Model+ post-processing (PFS)
Grid based	Yes	No	Yes	Yes
Variogram	Yes	No	No	Yes
Shape control	No	Yes	No (not good control)	Yes
№ of channels	No (proportion of cells)	Yes	No (proportion of cells)	Yes
Width/height	No (poor, only by variogram)	Yes	No (poor)	Yes
Local orientation	Yes	Yes	?	Yes

Objects can be simulated in space based on local or regional characteristics, such as density, orientation, size, etc. Therefore, most of the times objects are generated or simulated in space conditioned to stochastic measurements and characteristics extracted from well or seismic data. Simulation of channels in 3D space is adequate for object modelling procedures, as channels follows a complex geometry and the shape behaviour cannot be fully characterized only by two-point statistics. However, an object model of channels, even if conditioned to experimental statistics of shape and density, is not realistic and must be post-processed.

To generate realistic 3D morphological models for fluvial sand channels reservoirs, the idea of the proposed methodology is to combine object and geostatistical simulation models to generate a set of equally probable scenarios. Those scenarios can be filled with petrophysical properties in a second step.

4.1 Methodology

The workflow of the proposed methodology is represented in the figure 4.1 and is detailed next.

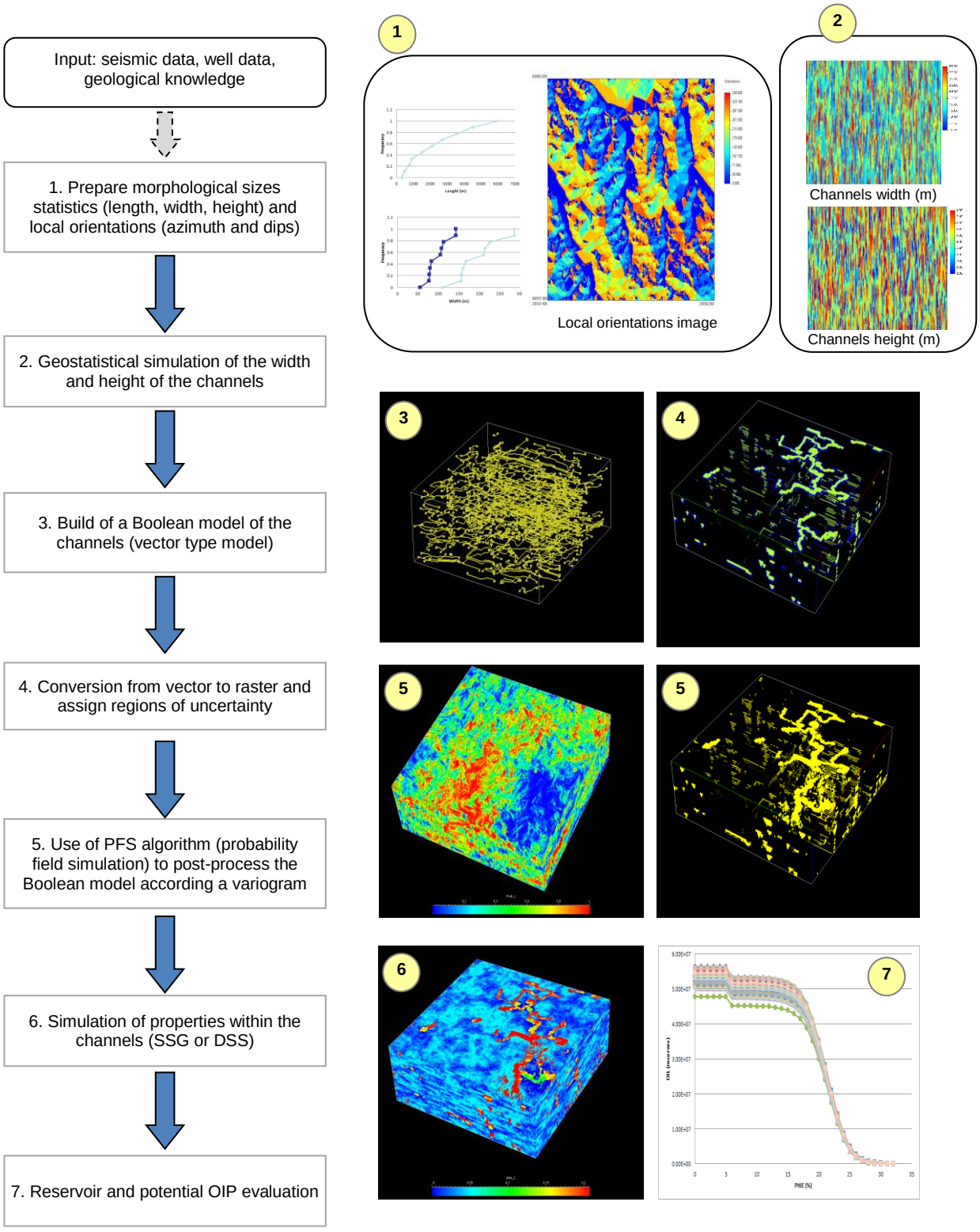

Figure 4.1 – Workflow of the proposed methodology.

Step 1: Data preparation. Input data for this flowchart consists of channels measurements (length, width and height), channels density and local channels orientation. Sizes can be considered by synthesis statistics (mean and variance under a distribution law) or for instance by cumulative histograms. A coefficient of correlation between channel width and height sizes can also be used. Channels density can be expressed as a fraction of channels volume by region, level or whatever. Local channels orientations are local azimuths and dips angles of the channels skeleton (See example for azimuths in figure 4.2). All those starting data can be obtained by geology expertize, similar geological formations, seismic interpretation together with well data (cores and logs) if available.

The relationship between channels measurements and channels density conditions the number of channels to be simulated within a specific volume. Local channels orientation conditions the sinuosity of the channels and the reciprocate connectivity. If local orientations are provided only at some locations, it is prior necessary to interpolate (for instance by kriging) both angles (azimuth and dip) into a 2D or 3D grid according the reservoir grid block model.

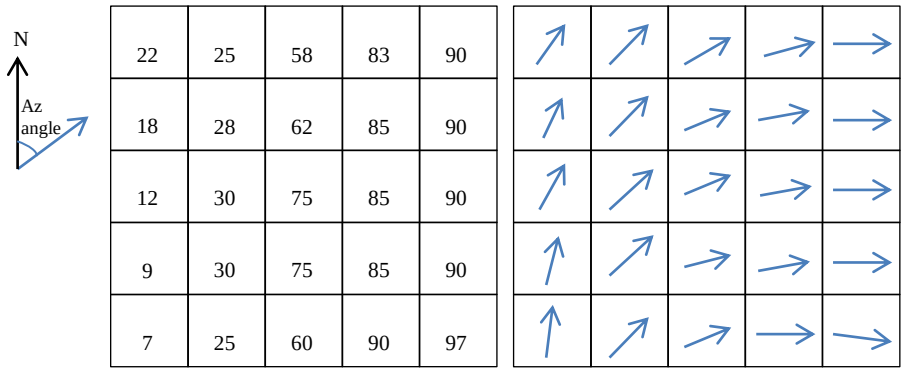

Figure 4.2 – Example of an image of local orientations (azimuths).

Step 2 Geostatistical simulation of the width and height of the channels. The objective of this step is to provide a pseudo-continuous value for the width and height of each channel to be simulated, conditioned to the histograms of width and height mentioned in the previous step. In the present work, it is proposed to simulate those values with Sequential Gaussian Simulation (SGS) or Direct Sequential Simulation within a synthetic 2D grid. Each column of this grid represents a hypothetical channel to be simulated and the rows represent the channel discretization in accordance with the reservoir grid block model. Thus, this 2D grid should be initiated with the number of columns equal to the maximum number of channels to be simulated and the number of rows equal to the maximum length of the channel divided by the reservoir grid block size.

For simulation, variogram between columns should be a pure nugget effect (no relationship between channels size) and between rows a range and a theoretical function must be considered. A relationship between widths and heights can be imposed if simulation of heights (or widths) are constrained to each other, for instance, using a co-simulation procedure (Co-DSS).

Step 3: Build of a Boolean model of channels. In this step, an object or Boolean model of the channels is generated following a vector structure of the data. In section, channels can be modelled by simple figures such as rectangles, half circles (width equal to height) or half ellipsoidal shapes, which was the approximation adopted in the present case study. Generation / simulation is performed channel by channel: a) generate a maximum length for the channel by Monte Carlo simulation from lengths histogram; b) random generation of an initial point location of the channel; c) from the initial point, grow skeleton of the channel for both sides, according local orientation angles plus a tolerance, and until channel reaches the predefined maximum length or the boundaries of the reservoir (see figure 4.3 left); d) select a trace of widths and heights simulated in the previous step and evaluate the volume of the channel assuming a U shape (see figure 4.3 right); e) simulate new channels using the same procedure until a previously defined objective in terms of channels proportion is reached. Output of this step is a set of arcs each of them represents the skeleton of a channel.

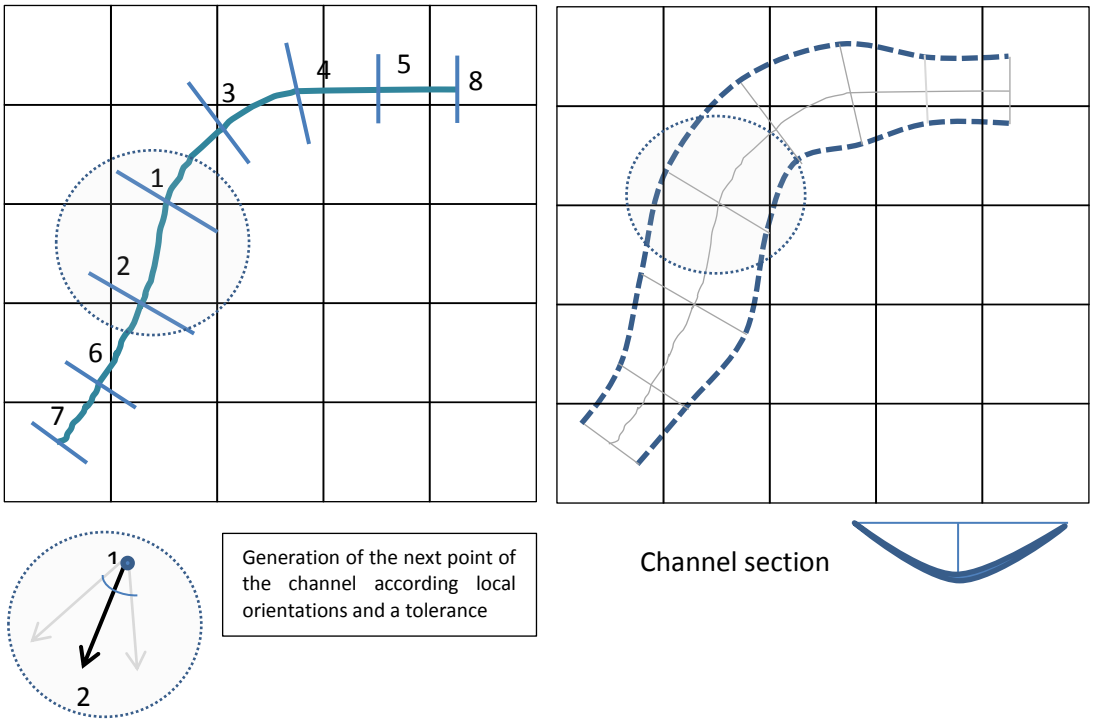

Figure 4.3 – Generation of a 3D channel: (left) simulation of the skeleton; (right) assign local widths and heights.

If well data is available, the simulation of the skeleton of the channels should begin from the well location, and in this case the exact location of the channel can be ajusted acording the height measure at the well and the height obtained by simulation. From this initial point, channels should increase from both sides until the objective-simulated length is achived. In these cases the post processing PFS keeps blocks classified as channels acording the well data.

Step 4: Conversion from vector to raster and assign regions of uncertainty. In this step, arcs from previous step, plus width and height local measurements are converted into a raster representation. Conversion identifies reservoir blocks where their centre is close to the skeleton according the local width and height values. Skeleton is considered located at the top of the channel, and channels have a U shape. Reservoir blocks are coded in three categories: within channel (sand), outside channel (shale) and transition between sand / shale (figure 4.4).

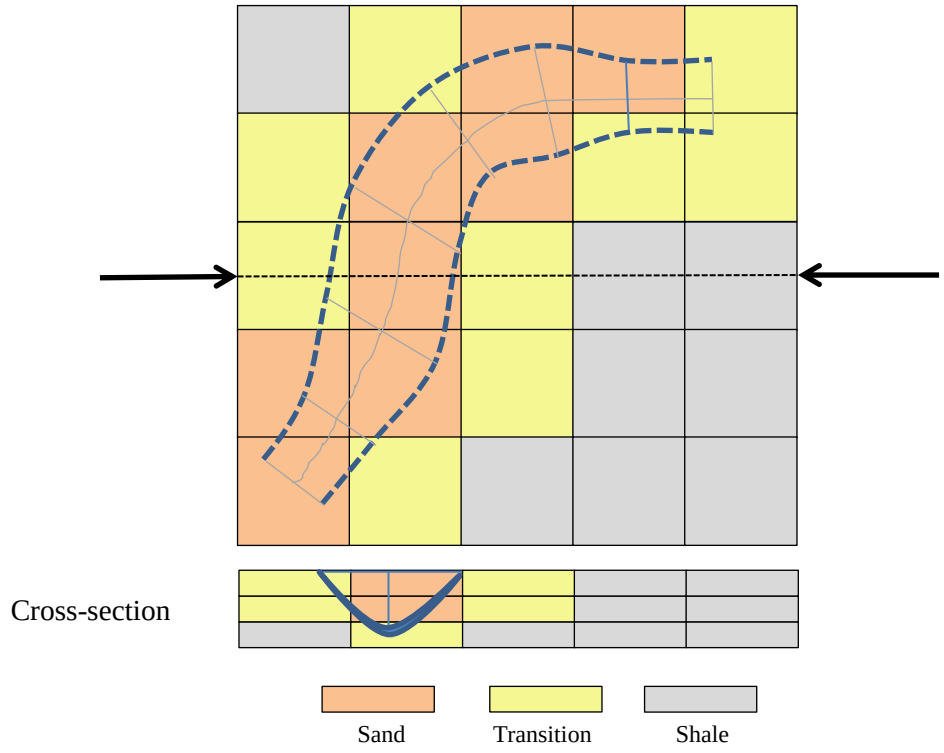

Figure 4.4 – Transformation from vector to raster and generation of three a priori regions (sand, transition and shale).

Step 5: Use of the Probability Field Simulation algorithm (PFS) to post-process the Boolean model according a variogram. In this step, the raster representation of the object channels model (with 3 regions, see previous step) is transformed into a binary map (channel – sand / not channel – shale) making use of a PFS procedure. It includes the following procedures: a) define a prior table

for transformation of values, meaning the probability of each a priori region became a channel (sand facies); b) simulate an image of Gaussian values conditioned to a variogram model and the local orientations of the grid; c) transform the Gaussian map into a probability map; d) apply the PFS and get final images of the sand / shale geometry.

Step 6: Simulation of properties within channels. Making use of the previous simulated images of channels, it is possible to generate properties within and outside the channels, such as porosity and permeability, if well data and histograms are available. In the present thesis, and only for demonstrative purposes, porosity values are generated by Direct Sequential Simulation (DSS) with regional histograms.

Step 7: Reservoir and potential OIP evaluation. In this final step, and also for demonstration purposes, curves of potential Oil in Place (OIP) calculated with porosity grids are presented.

4.2 Background of geostatistics

Geostatistics is a branch of statistics dealing with the problems associated with space (and / or time), and aims to characterize the spatial distribution (and / or temporal) of measured and present their local and global uncertainty, taking into regard a density, zoning and heterogeneity of the available information (Soares, 2006).

The geostatistics background was first proposed by Matheron, in sixties of the last century, with the characterization of mineral deposits. Later, geostatistics were extended for the characterization of oil reservoirs, natural resources and environmental problems, since all these phenomena are characterized by variables which are governed by the same statistical principles.

In summary, the use of geostatistical methodologies involves the three issues:

a) Data analysis;

b) Spatial analysis (calculation and fitting of experimental variograms);

c) Forecast (kriging estimation and/or simulation).

The basic paradigm of geostatistics is to convert the hypothetical value of each location x not sampled in a realization of a random variable$Z(x)$, whose distribution law allows us to understand and model the spatial variability.

A random variable (Z) is a variable that can assume a set of values (z) according a distribution law. The random variable (Z), or more specifically the distribution law, is dependent of the location, and that's why it is usual to present $Z(u)$ associated to a location u. The random variable is also dependent of the known information, which means, the distribution law changes when the information of the not sampled location $z(x)$ increases.

Random variables can be categorical or continuous. Lithology, facies and colours are examples of categorical variables; petrophysical properties (porosity, permeability and density), grades and geographical properties (elevation, thickness and depths) are examples of continuous variables.

The cumulative distribution function (*cdf*) of a continuous random variable $Z(u)$, can be expressed by:

$$F(u;z) = Prob\{Z(u) \leq z\}$$

When the *cdf* is presented for a location u, taking into account a set of n neighbour samples of location u, $Z(u_\alpha) = z(u_\alpha), \alpha = 1,\dots n$ it is used the designation "conditional to":

$$F(u;z|(n)) = Prob\{Z(u) \leq z|(n)\}$$

In geostatistics, most of the information related with an unsampled location $z(u)$ is given by the neighbour samples u' of the same attribute z or another y if correlated. Thus, it is important to model the correlation or dependence between the random variables $Z(u_\alpha) = z(u_\alpha), \alpha = 1,\dots n$ and $Z(u_\alpha) = z(u_\alpha), \alpha = 1,\dots n, Y(u_\beta') = y(u_\beta'), \beta' = 1,\dots n'$.

A random function is a set of random variables defined for the same area in study $\{Z(u), u \in study\ area\}$.

As a random variable is characterized by their *cdf*, a random function is characterized by the set of *K- cdf* given for K locations, $k = 1, \dots K$.

$$F(u_1, \dots, u_k; z_1, \dots, z_k) = Prob\{Z(u_1) \leq z_1; \dots; Z(u_k) \leq z_k\}$$

As a univariate *cdf* of the random variable $Z(u)$ is used to characterize the uncertainty of z(u), the multivariate *cdf* is used to characterize the joint uncertainty of the K values $z(u_1), \dots z(u_k)$.

The geostatistical methods presuppose that the random variables present simultaneously:

- A random pattern, which means, for small distances random variations exists;
- A structured pattern and, therefore, predictable (geology, grades dispersion).

The random component may be more or less predominant, associated with the variability of the phenomenon and their sampling, such as errors due to data collection, or the existence of different procedures for the quantification of the same attribute.

The geostatistics assumes that the statistical distribution of the difference of values of a variable between pairs of points (samples) is similar in all study area and depends only on the distance and orientation of pairs of points. This assumption is a designation of stationarity (2^{nd} order), and is the fundamental concept assumed in geostatistics. In summary, classic statistic does not take into account the location of the samples, and the geostatistic uses the location of each sample in relation with the neighbour samples.

This leads to the concept of a regionalised variable, which is a variable defined at a specific location of the study area that depends of the magnitude and the sample size (volume, shape and orientation). Typical examples of regionalised variables that can be worked with geostatistics are, for example, the thickness of a mineralized body, the bulk density, and physical parameters of the rock porosity, etc.

Given the impossibility of fully evaluate, in space and / or time, the distribution of the property in study, the characterization is usually based on a limited set of data obtained by several samples. The data collection presents specific characteristics associated with a certain degree of uncertainty and unique achievements making it impossible to repeat the observation in a given space and time.

Validation of the geostatistical models used in the characterization of the resources it will need to be made a posteriori by the intersection between the results obtained through modeling and the available data, which determines a greater or lesser distance (error) to reality.

In geostatistics are considered two evaluation strategies: estimation and simulation (Deutsch and Journel, 1992; Goovaerts, 1997; Soares, 2006). The estimation models or geostatistical interpolation are based on the formalism of kriging and aim to obtain an average picture of the phenomenon (variable) in the study. There are several variants of kriging (ordinary, simple) or kriging that consider the indirect information (cokriging, collocated cokriging, kriging with an external drift), or that are applied to categorical variables (indicator kriging) or continuous.

In estimation, we want to make the best possible estimate at the unsampled location via kriging, by minimalizing the error variance. However, there is no guarantee that the map obtained using kriging has the same variogram and variance as the original data.

The simulation models are to obtain a set of images as a whole that equiprobable quantifies of a local and global uncertainty. It allows us to come up with theoretically an infinite number of realizations of the map each of which has approximately the same variogram and variance of the original data.

One important use of simulation is in the petroleum industry. Simulated images allow petroleum engineers to have a range of fluid flow predictions all of which are plausible given the uncertainty in the distribution of the geological properties.

4.3 Spatial continuity and variograms

4.3.1 Variogram and spatial continuity

The dependence between observations can be evaluated with the variogram tool, which is a spatial correlation measurement by reference to a vector $\vec{h}$. The experimental variogram $\gamma(\vec{h})$ is calculated by the half-sum of the squares of differences between pairs of measurements in the direction of the vector $\vec{h}$ and separated by $|\vec{h}|$, where $N(\vec{h})$ is the number of pairs of points separated by a vector $\vec{h}$.

$$\gamma(\vec{h}) = \frac{1}{2N(\vec{h})} \sum_{\alpha=1}^{N(\vec{h})} \left[z(u_\alpha) - z(u_\alpha + \vec{h})\right]^2$$

For a specific direction, or set of directions, the values of $\gamma(\vec{h})$ are usually represented graphically with the distance (module of vector $\vec{h}$). The increment of $\gamma(\vec{h})$, with the distance, depends of the gradient of a sample value changes related with the distance. When $\gamma(\vec{h})$ stabilizes the maximum correlation distance is reached.

Another measurement of spatial continuity is the spatial covariance which can be calculated by:

$$C(\vec{h}) = \frac{1}{N(\vec{h})} \sum_{\alpha=1}^{N(\vec{h})} z(u_\alpha).z(u_\alpha + \vec{h}) - m_{-\vec{h}}.m_{+\vec{h}}$$

Where $m_{-\vec{h}} = \frac{1}{N(\vec{h})}\sum_{i=1}^{N(\vec{h})} z(x_i)$ and $m_{+\vec{h}} = \frac{1}{N(\vec{h})}\sum_{i=1}^{N(\vec{h})} z(x_i + \vec{h})$ are the left and right averages regarding vector $\vec{h}$, respectively.

The spatial covariance $C(\vec{h})$ is related with the variogram $\gamma(\vec{h})$ by $\gamma(\vec{h}) = C(0) - C(\vec{h})$ where $C(0) = C(|\vec{h}| = 0)$ is the statistical variance of the data.

4.3.2 Fitting of theoretical models

The experimental variograms obtained for different directions, from the information available, allow analysis of the structure of continuity of the variable under study. These experimental

variogram estimators can be interpreted as a comprehensive theoretical model, calculated only for some ranges of distance and directions. For this reason, the experimental variogram must be fitted by a theoretical function satisfying the requirement of being positive definite.

The theoretical model can be defined by a unique function, or a sum of theoretical functions as the sum of two positive-defined functions is still a function defined positive. The final model can be isotropic or not, as it is constant or not, according to the various directions.

The most common theoretical function is designated by spherical or Matheron. The growing behaviour of this function is more pronounced for shorter distances and then more slowly to reach a plateau (sill).

$$\gamma^*(h) = \begin{cases} C\left[1.5\frac{h}{a} - 0.5\left(\frac{h}{a}\right)^3\right] & if \;\; h \leq a \\ \\ C \quad otherwise \end{cases}$$

Where *C* is the sill (variance of the data), a is the range or maximum correlation distance and *h* is the distance.

Another widely used function is the exponential model.

$$\gamma^*(h) = C.Exp\left(\frac{h}{a}\right) = C\left[1 - Exp\left(-\frac{h}{a}\right)\right]$$

For all models it is also possible to add a nugget effect (C_0). The nugget effect can be interpreted as an indicator of the variability of the studied variable under the sampling distance.

Graphically, the nugget effect is represented as the ordinate at the origin of the graph representation of the semi-variogram versus distance. Theoretically can range between 0 (no nugget effect) and the sill of the variogram (pure nugget effect).

4.4 Simulation strategies

The models used in geostatistical modelling of phenomena are related to quantification of categorical and continuous variables describing natural resources that are possessed of a spatial structure, resulting from the association of behaviour with the theoretical foundations of mathematics and statistics, in particular the theory of random functions.

The choice of a particular geostatistical model should be based on the study and knowledge of the natural phenomenon in question, incorporating its spatial component in their characterization, which can be used for different applications in the areas of planning, recovery and monitoring the natural or more specifically geological resource. Validation of the geostatistical models is made a posteriori by the intersection between the results obtained by modeling and the available real data, which allows you to find a greater or lesser distance to the reality (space of uncertainty).

Geostatistical simulation is a stochastic process for generating images that reproduce the spatial distribution and uncertainty associated with different variables addressed in the Earth Sciences. This class of models aims to reproduce images of reality that reflect characteristics of the resource, such as the variability of the sample set, the distribution law of the variable under study, and spatial continuity. The result is a set of equiprobable images with the same spatial distribution of the experimental data, and reproduction of statistical and spatial variability quantified by the samples (histogram and variogram or spatial covariance). Typically, the simulation is not intended to obtain the average or the most likely characteristics of a given variable / resource (which is the objective of estimation), but a set of equiprobable images, enabling different views of a resource, and simultaneously quantify the uncertainty of these site characteristics given by the available data.

There are several simulation algorithms to generate images, but in this study sequential simulation and probability field simulation were used and therefore are described shortly below.

4.4.1 **Sequential simulation methods**

With a simulation model it is intended to reproduce in the simulated image, the variability of the phenomenon under study by two statistical measurements $Z(x) - F_Z(Z) = prob\{Z(x) < z\}$ – frequency of the classes histogram and the variogram $\gamma(h)$ that reproduces the spatial continuity of $Z(x)$.

If $Z_c(x)$ designates the simulated dataset, and $Z(x_\alpha)$, $x_\alpha = 1, \dots, n$, the n experimental values, the simulated images must fulfil the following itens:

1. For any value of z: $prob\{Z(x_\alpha) < z\} = prob\{Z_c(x) < z\}$.
2. $\gamma(h) = \gamma_c(h)$, where $\gamma(h)$ and $\gamma_c(h)$ are respectively the variograms of the experimental and simulated values.
3. At any experimental location x_α the know value $Z(x_\alpha)$ and the simulated value $Z_c(x_\alpha)$ matches: $Z(x_\alpha) = Z_c(x_\alpha)$. The simulated image has the same variability as the original data and matches the experimental known values.

The sequential simulation is based on the Bayes relationship, transforming the conditioning process as a simple and successive procedure that can be generalised by:

$$F(Z_1, Z_2, Z_3, \dots, Z_N) = F(Z_1)F(Z_2|Z_1)F(Z_3|Z_1, Z_2) \dots F(Z_N|Z_1, Z_2, \dots, Z_{N-1}).$$

If one consider a joint function of N random variables and n experimental and conditioning data $F(N) = \left(Z_1, Z_2, Z_3, \dots, Z_N\middle|(n)\right)$, to simulate a set of N values $z_1, \dots, z_N$ of $F(N)$, the full process can be summarised as this:

1. Simulation of a first variable z_1 from the cumulative distribution function $F(Z_1|(n))$. Once simulated, this variable will be conditioning data for the remaining values, and the conditioning information is increased from n to $n + z_1$;
2. Simulation of a second variable z_2, from the cumulative distribution function Z_2 now with $\{n + 1\}$ conditional variables; conditional information is updated to $(n + 2) = (n + 1) + z_2$;
3. Repeat the process until the sequence of N sequential simulated variables is complete.

It is important to mention that the N random and dependent variables $Z_1, Z_2, Z_3, \dots, Z_N$ can represent the same property spatially referenced in the N grid nodes of the studied area it is intended to simulate the same variable. Thus, for the n initial conditional values correspondent to the experimental data (x_α), $x_\alpha = 1, \dots, n$ the joint distribution law of the N random variables is $F(N) = \left(Z(x_1), Z(x_2), Z(x_3), \dots, Z(x_N)\middle|(n)\right)$.

The practical implementation of this procedure is limited by the unknown of the N conditional cumulative distributions law:

$$prob\{Z(x_1) < z|(n)\}$$

$$prob\{Z(x_2) < z|(n+1)\}$$

$$prob\{Z(x_3) < z|(n+2)\}$$

$$\vdots$$

$$prob\{Z(x_N) < z|(n+N-1)\}$$

Journel & Alabert, 1989 proposes the use of the kriging for the estimation of this conditional cumulative distribution laws, particularly the indicator kriging for categorical variables and the multiGaussian kriging for continuous variables. This approach leads to the sequential indicator

simulation (SIS) and sequential Gaussian simulation (SSG), for categorical and continuous variables, respectively (Nunes and Almeida, 2010).

As the sequence of the simulation of the N nodes is random, as well as the generation of the simulated value at each node using a Monte Carlo procedure, each realization is independent. All simulated images are equally probable, match the histogram, variogram and the original data at samples locations.

4.4.2 **Sequential Gaussian simulation**

The sequential Gaussian simulation (SGS) is a procedure where all values of the variable under study are prior transformed to a Gaussian distribution law, $Y(x) = \Phi[Z(x)]$, and all process is developed within a Gaussian framework (Journel, 1989). Back transform of the simulated Gaussian values for the original distribution law is performed at the end. It is a parametric approach in the sense that kriging estimates the local mean and variance of a Gaussian distribution type.

4.4.3 **Direct Sequential simulation**

For continuous variables, the Direct Sequential simulation (DSS), unlike SGS, uses the original variable without any previous transformation of the data. For instance, as SGS uses a prior transformation of the data to a Gaussian distribution, and a back-transformation at the end, it is sometimes difficult to reproduce the variograms of the original variable mainly for extremely skew distributions. This effect increases if secondary variables are used within a co-simulation procedure.

The DSS as proposed by Soares, 2001, uses the local mean and variance to resample the global cumulative distribution law $F_Z(z)$, and build a new local cumulative distribution function $F_Z^{'}(z)$ with intervals centred on the local estimated average and with a range proportional to the local conditional variance. Those two local parameters mean and variance are estimated by simple kriging:

$$[z(x_o)]^* - m = \sum_{\alpha} \lambda_{\alpha}(z(x_{\propto}) - m)$$

One way to define the intervals and get the simulated value $z^s(x_0)$ from $F_Z^{'}(z)$ is to select a subset of n contiguous values $z(x_i)$ of the global experimental histogram whose mean and variance of the selected values is equal to the local estimated mean $[z(x_o)]^*$ and estimation variance $\sigma_{ks}^2(x_0)$:

$$\frac{1}{n} = \sum_{i=1}^{n} [z(x_i) - [z(x_o)]^*]^2 = \sigma_{ks}^2(x_0) \qquad and \qquad \frac{1}{n}\sum_{i=1}^{n} x(x_i) = [z(x_0)]^*$$

Another way to define the function is to use a Gaussian distribution law only as a helper function to re-sample intervals $F_z(z)$ and not to transform the original data to Gaussian distribution.

The following sequence of steps summarizes the simulation of a variable $z(x_0)$ via SSD:

1. Define a random path visiting each node of a regular grid of nodes.
2. At x_0, node to be simulated, kriging estimation of the local mean $z(x_0)^*$ and variance $\sigma_{sk}^2(x_u)$ conditional to the experimental data and the nodes previously simulated.
3. Definition of the intervals for resampling of the global distribution law $F_Z(z)$, by a Gaussian transformation $G([y(x_0)], \sigma_{ks}^2(x_0))$, where $[y(x_0)]^* = \varphi([z(x_0)]^*)$, φ being the normal score transform of the variable.
4. Calculation of the simulated value $z^s(x_0)$:
    a. Generate a value p from an uniform distribution $U(0,1)$,
    b. Generate y^s through $G\left(y(x_0)^*, \sigma_{sk}^2(x_0)\right)$,
    c. Return of the simulated value $z^s(x_0) = \varphi^{-1}(y^s)$.
5. Repeat steps 2-5 until all nodes are simulated.

To highlight the contract between properties within and outside the channels, and to avoid to run two simulations of properties, for the simulation of the porosity conditioned to the facies presented in the last part of the case study, the histograms used for resampling are not the global histogram but two local histograms, one for channel data and another for not channel data (Roxo, 2011).

4.4.4 **Probability field simulation**

Once allocated a priori probability of each grid node x_0 belonging to a channel (output object based model) via regions or classes (*cl*) of uncertainty (*ncl*=3 in the present case study) (*cl*=1 high probability of being a channel; *cl*=2 50% of being a channel and *cl*=3 low probability of being a channel), the Probability Field Simulation (PFS) step of the proposed methodology (Srivastava, 1992, Froidevaux, 1993) has the objective of reclassify the a priori probabilities into a binary image (channel / not channel). This procedure transforms the object-based model (smooth shapes) into a more realistic model imposing a theoretical model of variogram.

In particular, for each location x_u the cumulative distribution function corresponding to the class *cl* allocated to x_u is known:

$$F_Z(x_u, c) = Prob\{Z(x_u) < z \mid c = cl\}, cl = 1, \dots ncl$$

If a probability field image $P(x)$ is generated for the entire area A thus the simulated value $Z_s(x_u)$is equal to:

$$Z_s(x_u) = F_z^{-1}(x_u, c, p) \text{ where } p = P(x_u)$$

The probability field image can be generated by simple transformation of a Gaussian image provided by a geostatistical simulation algorithm for continuous variables, such as SGS or the turning band method.

In this particular case study, the probability field map is generated regarding local orientations of the covariance (Soares, 1990) (figure 4.5).

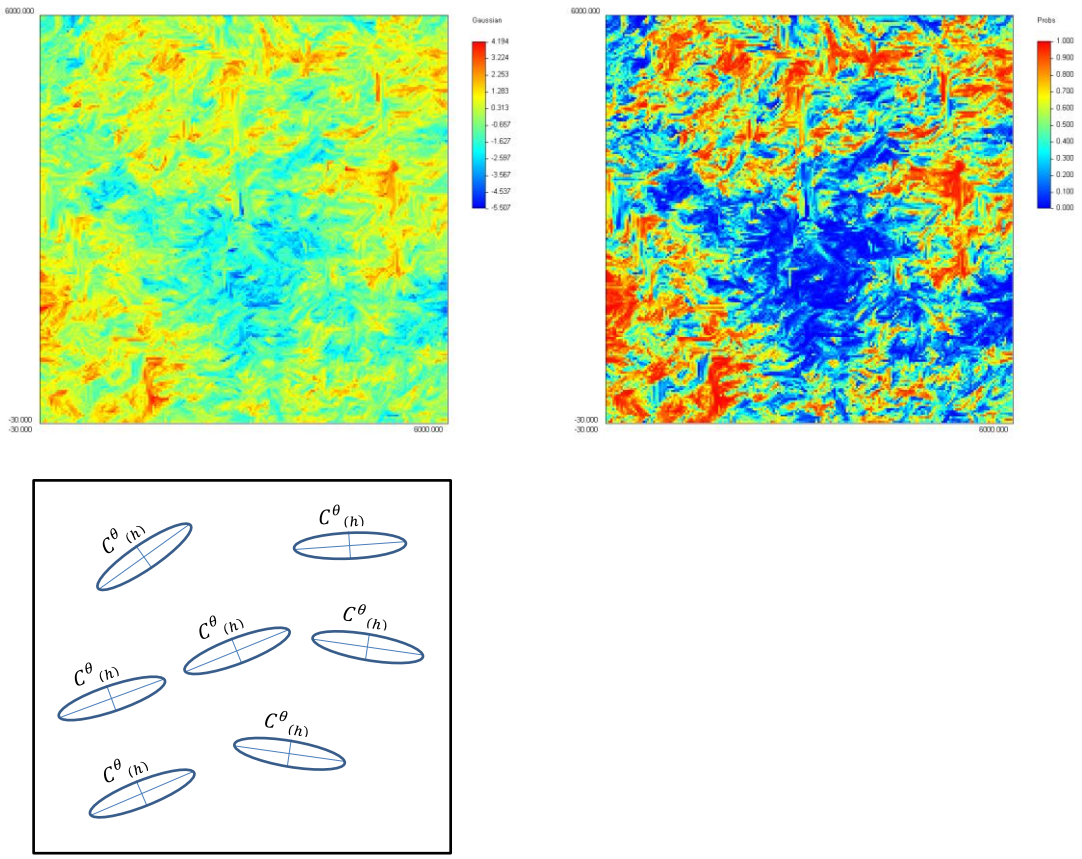

Figure 4.1 – (top left) Simulated image of gaussian values conditioned to local ellipsoid orientations ; (top right) Homologous probability field simulated image; (bottom) local ellipsoid orientations (only for illustrative purposes, no correspondence with the top images).

To apply local orientations, the covariances of the right matrix of the kriging system are rotated of θ degrees, which is the angle of the main direction of the ellipsoid of anisotropy in the location to estimate / simulate.

5. CASE STUDY

A stochastic methodology for modelling fluvial reservoirs composed of discontinuous sands is presented in previous section. A synthetic case study for demonstrative purposes is presented in this section.

5.1 Starting data

Reliable statistical starting data is a pre-requisite of successful probabilistic modelling of fluvial reservoirs. Starting data for the proposed morphology consists of:

a) Histogram of lengths;
b) Histogram of widths and heights and a ratio or a correlation coefficient width-height;
c) Images of the local orientation angles (azimuths, 2D and dips, 3D).

In real case studies, this information should be provided by geological expertise, seismic or other sources.

For modelling purposes, it was initiated a synthetic grid of blocks with the characteristics listed in table 5.1.

Table 5.1 – Parameters of the synthetic reservoir grid blocks.

	X direction	Y direction	Z direction
Number of blocks	200	200	30
Block sizes (m)	30	30	2
Initial coordinates	0	0	0

Concerning lengths, widths and heights (dimensions of the channels), three cumulative histograms were initiated (figure 5.1). Lengths range between 300m (10 grid blocks) and 6000m (maximum size of the studied area); widths range between 110m (3-4 grid blocks) and 285m (approximately minimum length of the channels); and finally heights range between 2 (one reservoir block) and 8 meters (4 reservoir blocks). A relationship between width and height dimensions via a correlation coefficient was used.

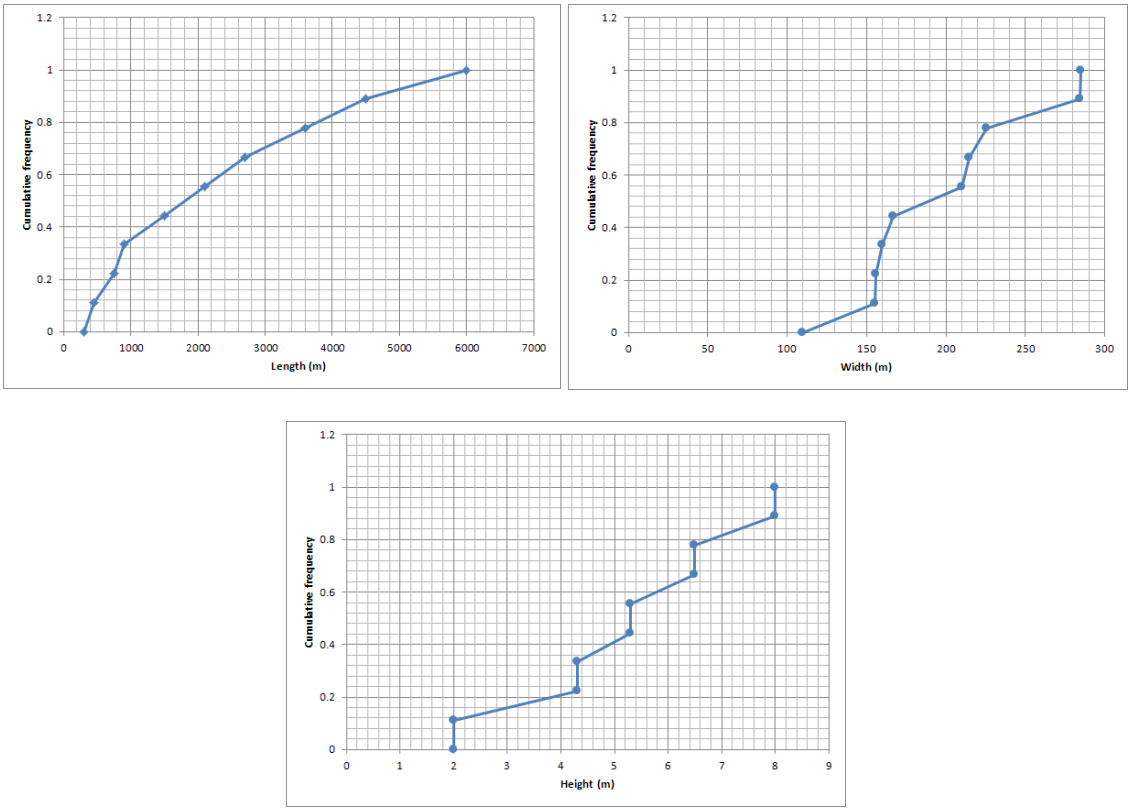

Figure 5.1 – Cumulative histograms of the length, width and height dimensions.

For this study, an image of the local directions of flow (angles relative to the North) was also constructed. This image was built on ArcGIS from a digital terrain model where hydrological functions such as FILLMDT and FlowDirection were applied (figure 5.2).

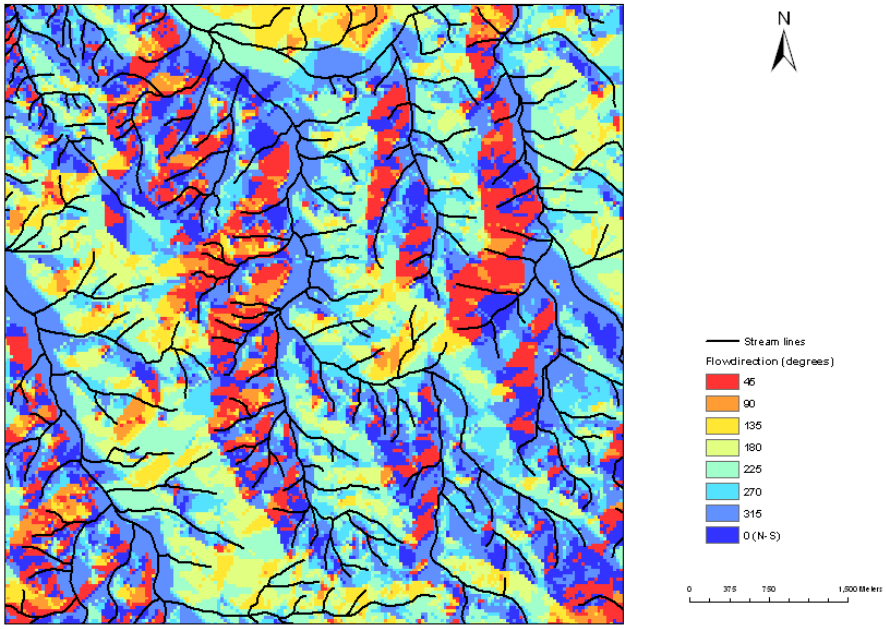

Figure 5.2 – Flow direction angles or local orientation of the potential flow (Aljustrel, Alentejo).

For the simulation of channels this image was pre-processed resulting in the figure 5.3

a) Values were smoothed by a 3x3 average filter as the *flowdirection* function intends to generate thin streamlines with one cell width (*flowaccumulation* function), therefore for wider geobodies such as sand channels this smoothing step was considered;
b) As only directions are needed for simulation, values were reclassified within an interval between 0 and 180 degrees.

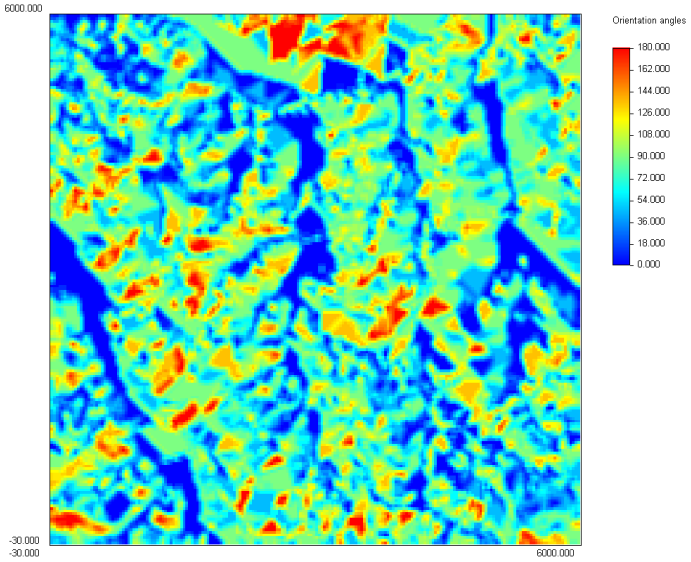

Figure 5.3 – Flowdirection angles after smoothing and reclassification.

For comparison purposes, three scenarios of simulation were developed and are presented:

a) Generation of 250 channels within the studied volume;
b) Generation of 500 channels within the studied volume;
c) Generation of 500 channels within the studied volume where initial widths values were subdivided by two.

5.2 Stochastic simulation of width and height dimensions

The first processing step consists of the simulation of width and height dimensions of the channels. The generation was done by conditional simulation (DSS) with the histograms of Figure 5.1, and a correlation coefficient of 0,7 between height and width dimensions. Two realizations of each are generated respectively for 250 and 500 channels. A spherical variogram model with 1200 meters range was used in all simulations. Figure 5.4 and 5.5 shows one realization for width and height dimensions (each column of values represents a channel, rows values within each column

represents dimensions throughout each channel) for 250 and 500 channels. Table 5.2 lists the average dimensions (width and height) of the simulated scenarios considered in this study.

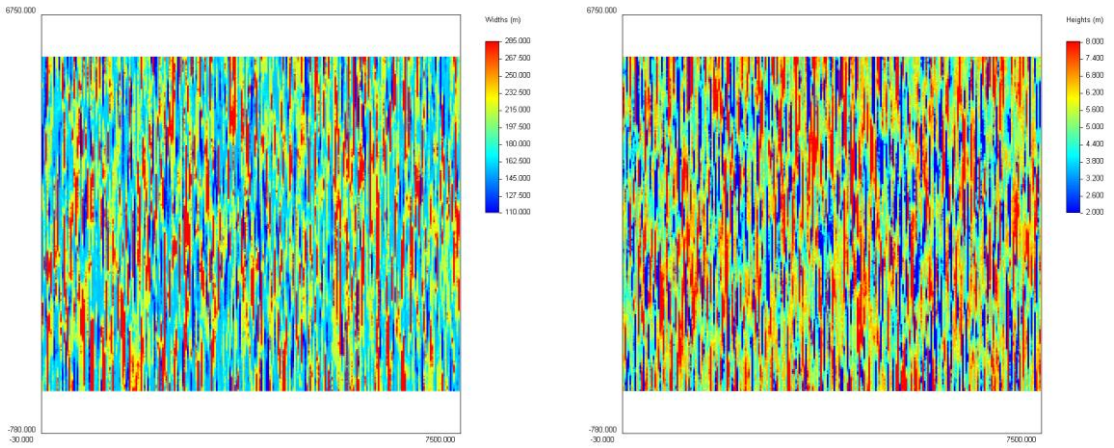

Figure 5.4 – (left) Simulated values of widths for 250 channels; (right) simulated values of heights for 250 channels.

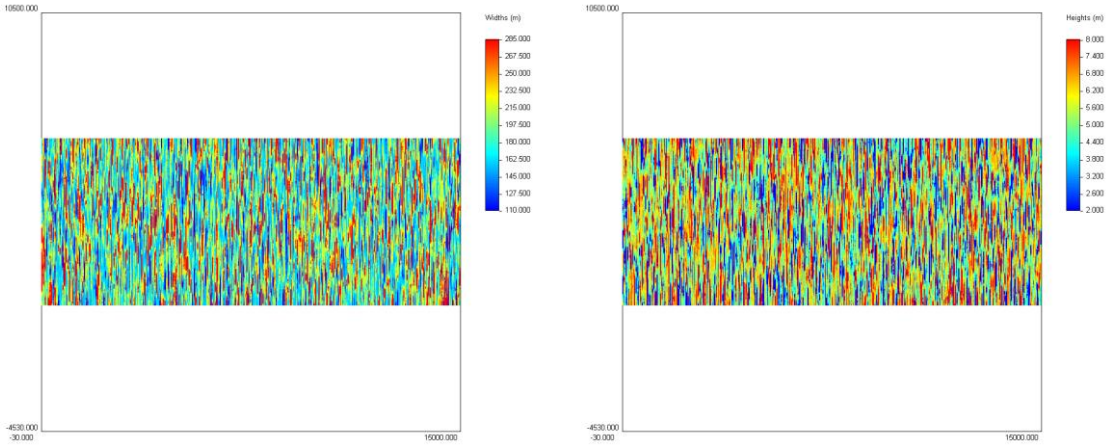

Figure 5.5 – (left) Simulated values of widths for 500 channels; (right) simulated values of heights for 500 channels.

Table 5.2 – Average dimensions of the channels.

Realisation	**Average width (m)**			**Average height (m)**	
	250 channels	500 channels	500 channels, width /2	250 channels	500 channels
#1	196,4	197,3	98,7	5,3	5,3
#2	197,2	195,3	97,6	5,2	5,2
Histogram		196,7		5,2	

All average values are similar between realisations and also similar to those obtained from the conditional histogram of figure 5.1.

5.3 Boolean model of the channels

Simulation of channels begins with a Boolean model as explained before. Fifteen realizations of skeletons were developed for each of the two dimension images and for 250 and 500 channels (initial width and width subdivided by 2). In total, 15 x 2 x 3 = 90 realizations were done. After the simulation of the skeletons, width and height dimensions were applied and three regions (predominant sand - red, transition - white and shale – transparent) were generated. Figures 5.6 through 5.8 illustrate images of skeletons respectively for 250 and 500 channels (base and half width) and the correspondent block model. Proportions for all simulations are listed in table 5.3, 5.4 and 5.5.

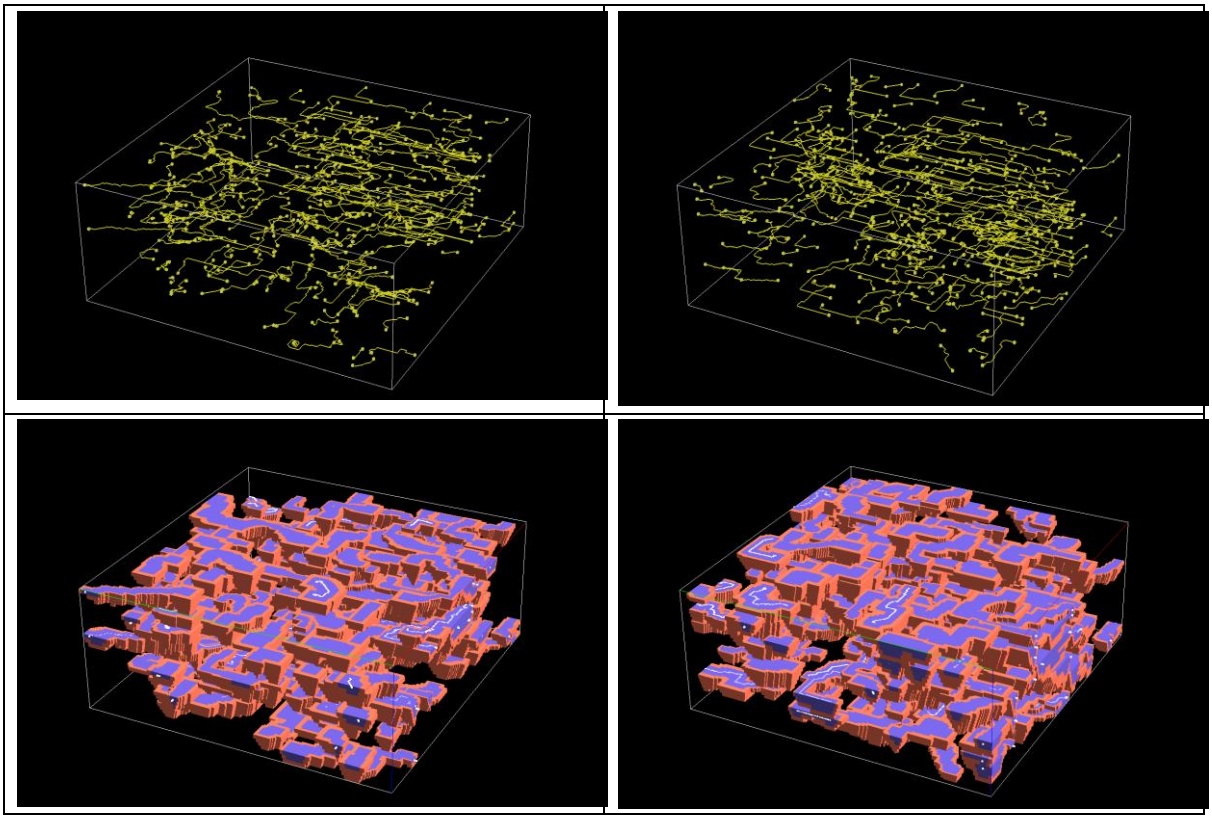

Figure 5.6 – (top) Two simulations of skeletons for 250 channels; (bottom) correspondent 3 regions block models (blue – sand; red – transition sand/shale).

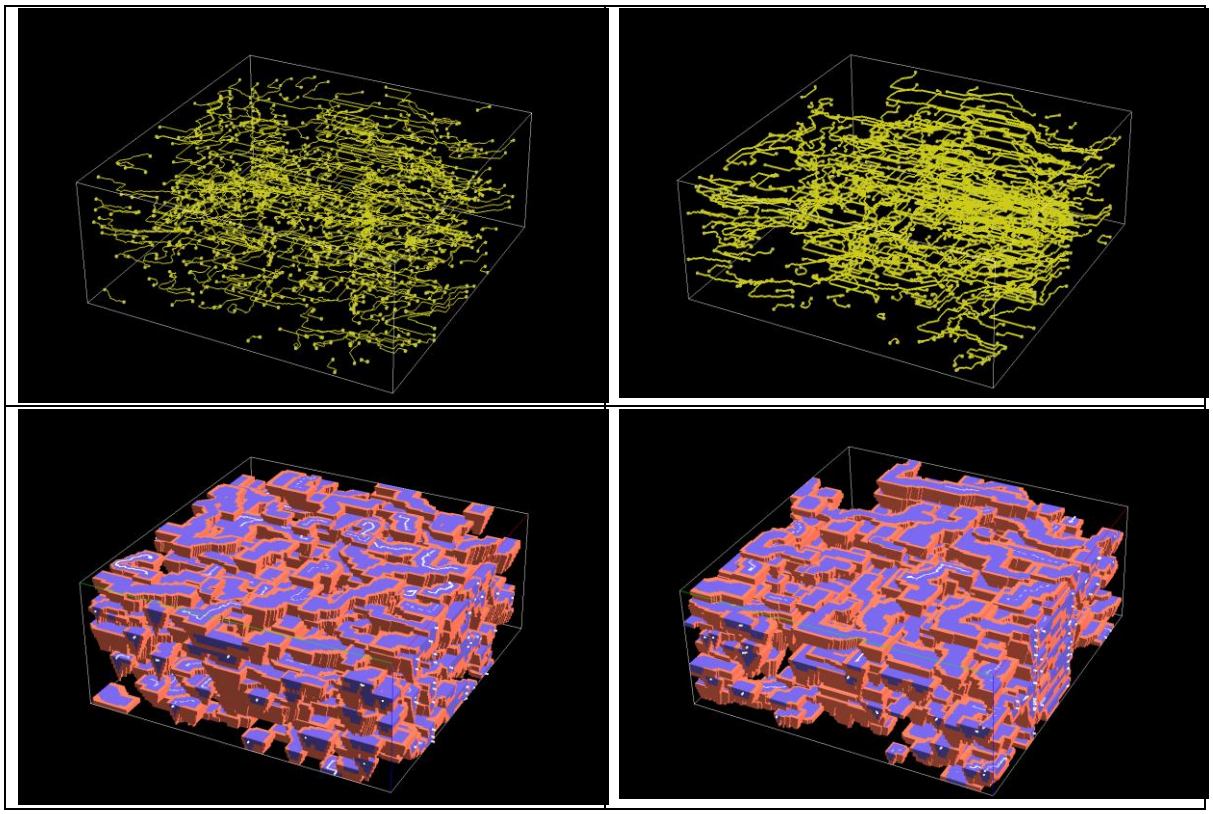

Figure 5.7 – (top) Two simulations of skeletons for 500 channels; (bottom) correspondent 3 regions block models (blue – sand; red – transition sand/shale).

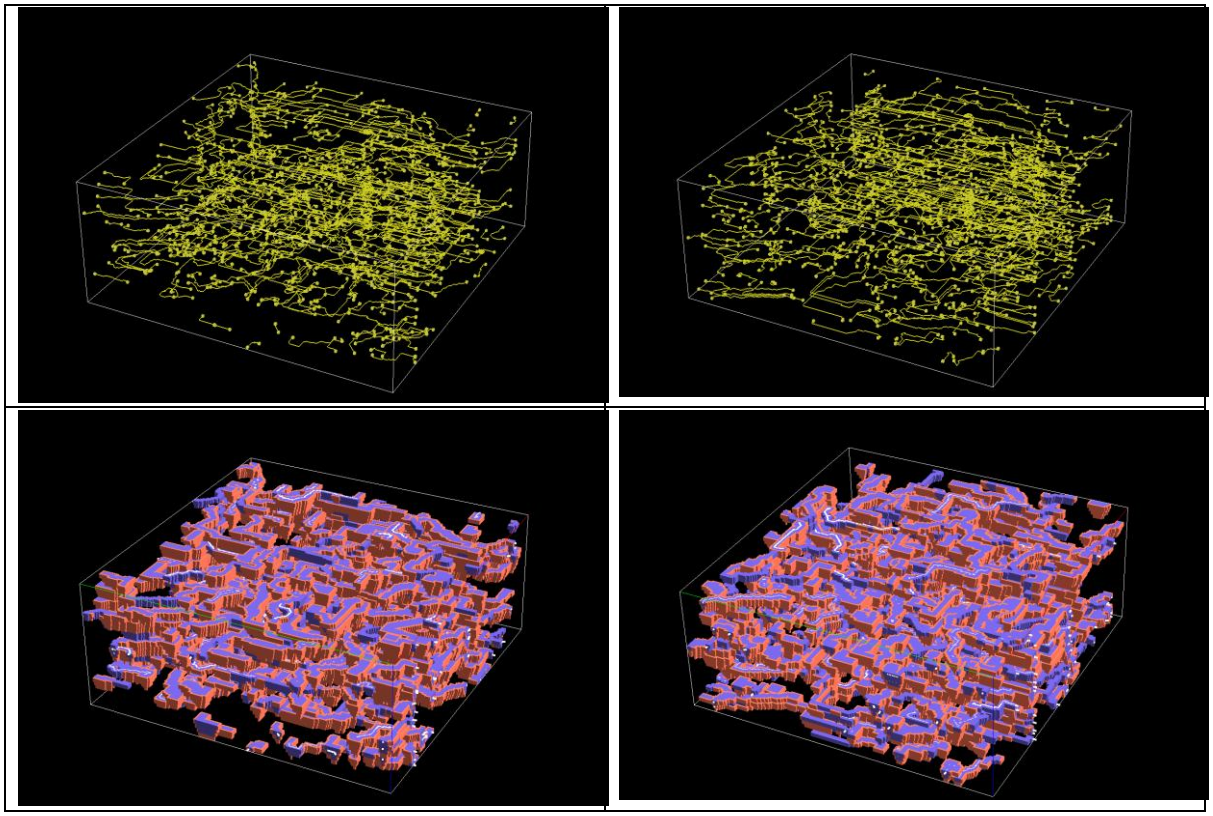

Figure 5.8 – (top) Two simulations of skeletons for 500 channels; (bottom) correspondent 3 regions block models (blue – sand; red – transition sand/shale) with width subdivided by two.

Table 5.3 – Proportions of the different regions (shale, sand, and transition shale-sand) by realization, scenario of 250 channels.

	250 channels, realization #1 of width-height			250 channels, realization #2 of width-height		
	Shale	Shale-Sand	Sand	Shale	Shale-Sand	Sand
1	0.758	0.112	0.130	0.739	0.123	0.138
2	0.726	0.128	0.146	0.742	0.121	0.137
3	0.749	0.118	0.134	0.757	0.115	0.128
4	0.745	0.120	0.135	0.759	0.115	0.127
5	0.743	0.121	0.136	0.755	0.114	0.132
6	0.744	0.120	0.135	0.756	0.114	0.130
7	0.749	0.119	0.132	0.740	0.120	0.140
8	0.744	0.119	0.137	0.729	0.126	0.145
9	0.749	0.118	0.133	0.757	0.112	0.131
10	0.753	0.116	0.131	0.748	0.116	0.136
11	0.760	0.112	0.128	0.749	0.118	0.133
12	0.742	0.120	0.138	0.744	0.120	0.136
13	0.756	0.112	0.132	0.751	0.118	0.130
14	0.736	0.124	0.141	0.752	0.116	0.132
15	0.745	0.120	0.135	0.754	0.115	0.131
Average	0.747	0.119	0.135	0.749	0.118	0.134

Table 5.4 – Proportions of the different regions (shale, sand, and transition shale-sand) by realization, scenario of 500 channels.

	500 channels, realization #1 of width-height			500 channels, realization #2 of width-height		
	Shale	Shale-Sand	Sand	Shale	Shale-Sand	Sand
1	0.578	0.216	0.206	0.572	0.216	0.212
2	0.563	0.220	0.217	0.573	0.217	0.210
3	0.577	0.210	0.214	0.579	0.213	0.208
4	0.565	0.221	0.214	0.571	0.220	0.209
5	0.573	0.214	0.213	0.566	0.217	0.217
6	0.576	0.212	0.212	0.566	0.218	0.216
7	0.575	0.214	0.211	0.586	0.209	0.205
8	0.556	0.227	0.218	0.564	0.220	0.216
9	0.568	0.216	0.215	0.573	0.217	0.211
10	0.590	0.206	0.204	0.583	0.210	0.207
11	0.578	0.213	0.209	0.569	0.218	0.213
12	0.573	0.216	0.211	0.566	0.219	0.215
13	0.591	0.209	0.199	0.575	0.216	0.209
14	0.581	0.213	0.206	0.582	0.214	0.204
15	0.578	0.216	0.206	0.582	0.209	0.209
Average	0.575	0.215	0.210	0.574	0.216	0.211

Table 5.5 – Proportions of the different regions (shale, sand, and transition shale-sand) by realization, scenario of 500 channels, width / 2.

	500 channels, realization #1 of width-height			500 channels, realization #2 of width-height		
	Shale	Shale-Sand	Sand	Shale	Shale-Sand	Sand
1	0.846	0.087	0.067	0.846	0.087	0.067
2	0.846	0.089	0.066	0.852	0.084	0.064
3	0.843	0.089	0.068	0.849	0.085	0.066
4	0.845	0.087	0.068	0.840	0.091	0.070
5	0.839	0.091	0.070	0.847	0.087	0.067
6	0.845	0.088	0.067	0.851	0.084	0.065
7	0.841	0.089	0.069	0.840	0.090	0.070
8	0.850	0.085	0.065	0.840	0.090	0.070
9	0.842	0.088	0.069	0.846	0.087	0.067
10	0.848	0.086	0.066	0.842	0.089	0.068
11	0.850	0.085	0.065	0.847	0.086	0.067
12	0.846	0.087	0.067	0.845	0.087	0.068
13	0.840	0.091	0.070	0.840	0.091	0.070
14	0.849	0.085	0.066	0.847	0.086	0.067
15	0.838	0.093	0.070	0.844	0.088	0.068
Average	0.845	0.088	0.068	0.845	0.087	0.068

5.4 Probability Field Simulation

Probability field simulation (PFS) algorithm was used for this next step of the methodology to post-process the object model and transform the transition zone conditioned to a variogram model. PFS begins with the simulation of a probability image with a uniform distribution law between 0 and 1. Sixty simulated images were generated and the first two are represented in figure 5.9. For demonstration purposes, theoretical model of variogram was defined in accordance with the dimensions previous proposed for channels: spherical model with 3000 meters in main direction, 200 m in the perpendicular at horizontal and 10m in vertical. As can be seen in the figure, probability maps follows the local orientations defined before.

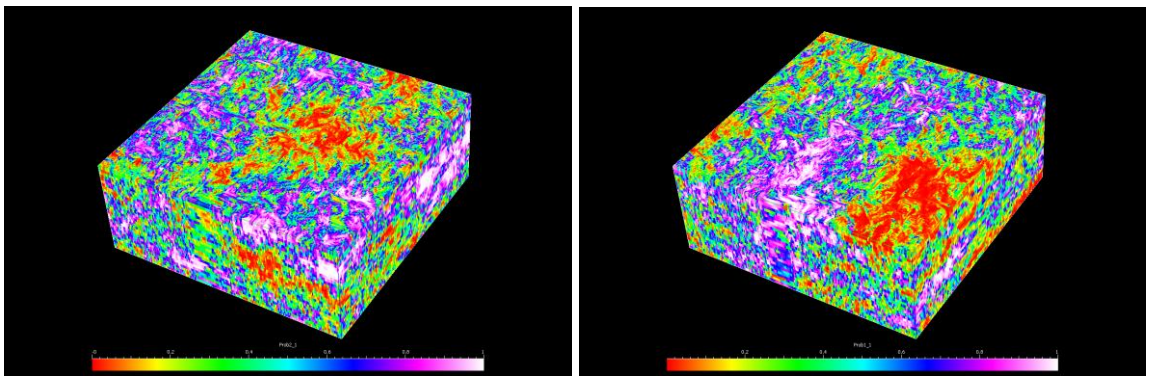

Figure 5.9 – Examples of two simulated probability images used for PFS purposes.

In a final step, PFS was applied for the simulation of shale / sand geometry conditioned to the a priori object model regions via the simulated probability maps with uniform distribution resulting in sixty simulated images of each scenario. To each region previously simulated it was assigned a priori probability of being sand (table 5.6). Figure 5.10, 5.11 and 5.12 show two examples of simulations for each scenario and tables 5.7, 5.8 and 5.9 the basic univariate statistics of the set of simulated images.

Table 5.6 – A priori probabilities of each region being sand / shale.

	A priori probability of being	
Object model regions	Sand	Shale
I - Shale	0,02	0,98
II - Transition	0,50	0,50
III - Sand	0,98	0,02

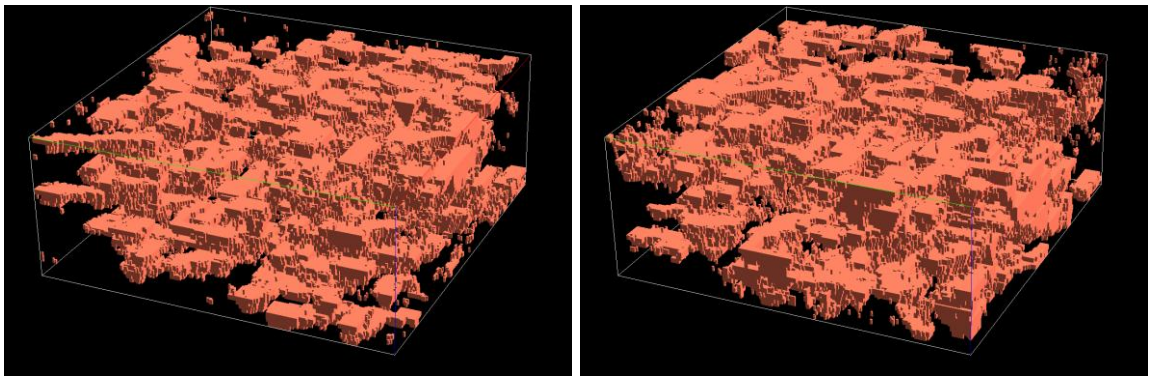

Figure 5.10 – Examples of two simulated images of the morphology of the sand / shale system for 250 channels.

Table 5.7 - Statistic results of the sixty simulated images, scenario of 250 channels (PFS).

	A priori probabilities from the PFS images			**Final shale/sand images**	
	Shale	Transition	Sand	Shale	Sand
Min	0.7257	0.1116	0.1268	0.7914	0.1807
Q1	0.7434	0.1149	0.1309	0.8055	0.1860
M	0.7488	0.1182	0.1333	0.8091	0.1909
Q3	0.7546	0.1203	0.1365	0.8140	0.1945
Max	0.7602	0.1284	0.1458	0.8193	0.2086

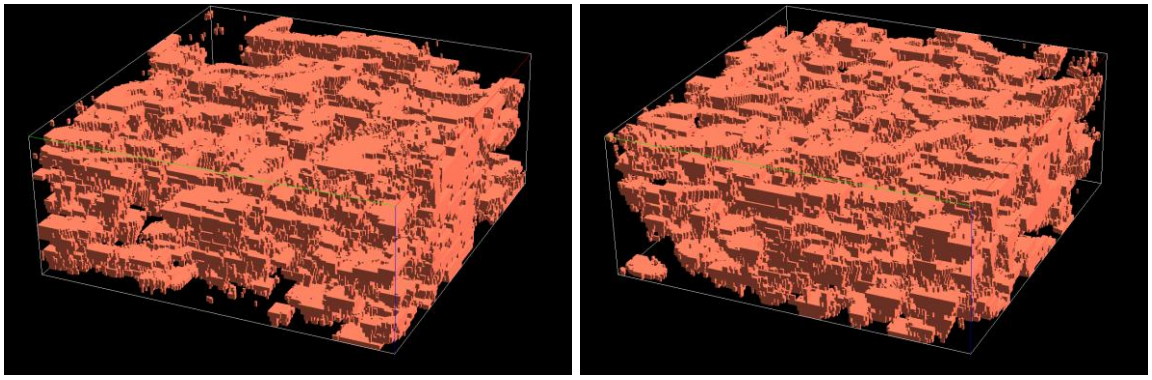

Figure 5.11 – Examples of two simulated images of the morphology of the sand / shale system for 500 channels (initial width).

Table 5.8 - Statistic results of the sixty simulated images, scenario of 500 channels (PFS).

	A priori probabilities from the PFS images			Final shale/sand images	
	Shale	Transition	Sand	Shale	Sand
Min	0.5556	0.2063	0.1995	0.6594	0.3126
Q1	0.5684	0.2129	0.2071	0.6706	0.3204
M	0.5742	0.2161	0.2106	0.6752	0.3248
Q3	0.5789	0.2179	0.2142	0.6796	0.3294
Max	0.5914	0.2266	0.2178	0.6874	0.3406

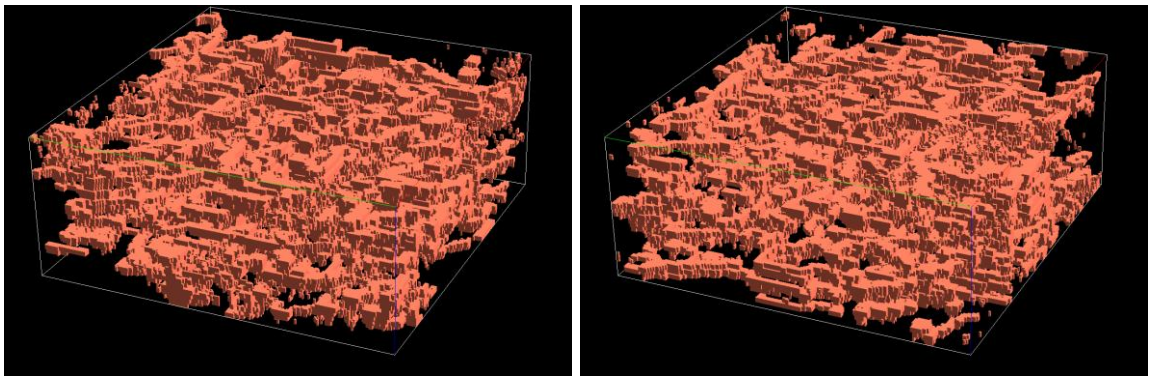

Figure 5.12 – Examples of two simulated images of the morphology of the sand / shale system for 500 channels (width / 2).

Table 5.9 - Statistic results of the sixty simulated images, scenario of 500 channels, width / 2 (PFS).

	A priori probabilities from the PFS images			Final shale/sand images	
	Shale	Transition	Sand	Shale	Sand
Min	0.8375	0.0837	0.0640	0.8641	0.1235
Q1	0.8416	0.0861	0.0663	0.8686	0.1273
M	0.8454	0.0872	0.0674	0.8711	0.1289
Q3	0.8471	0.0894	0.0694	0.8727	0.1314
Max	0.8517	0.0926	0.0701	0.8765	0.1359

5.5 Porosity simulation constrained to the shale / sand system

On base of the previous simulated images of channels (shale / sands), it is possible to simulate properties, such as porosity and permeability, if well data and / or histograms are available. To present this the following steps should be taken:

a) Prepare conditional histograms of porosity for the shale / sand regions (figure 5.13);

b) Simulate values of porosity.

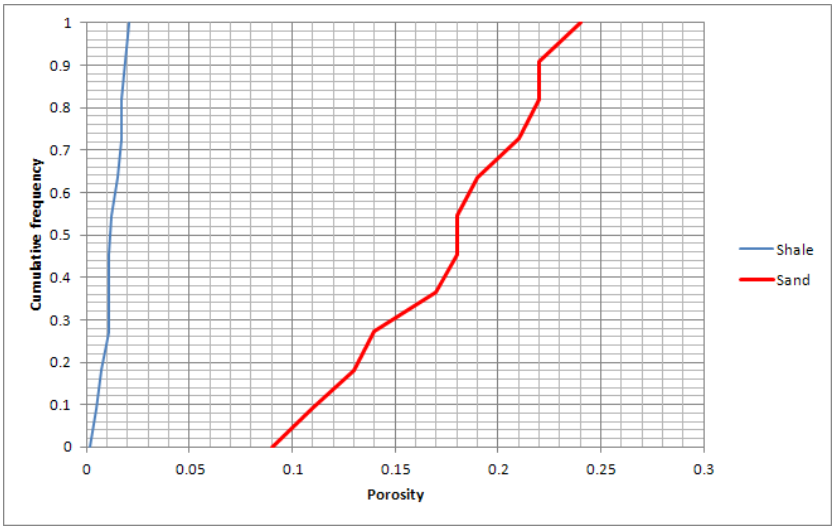

Figure 5.13 – Cumulative histograms for porosity conditioned to sand and shale facies.

In the present case study, and only for demonstrative purposes, porosity values are generated by Direct Sequential Simulation (DSS) with regional histograms. After the DSS procedure was received 180 images (60 images of each 3 cases). Figure 5.14 show one example of each conditioned to 250 channels, 500 channels (and width / 2).

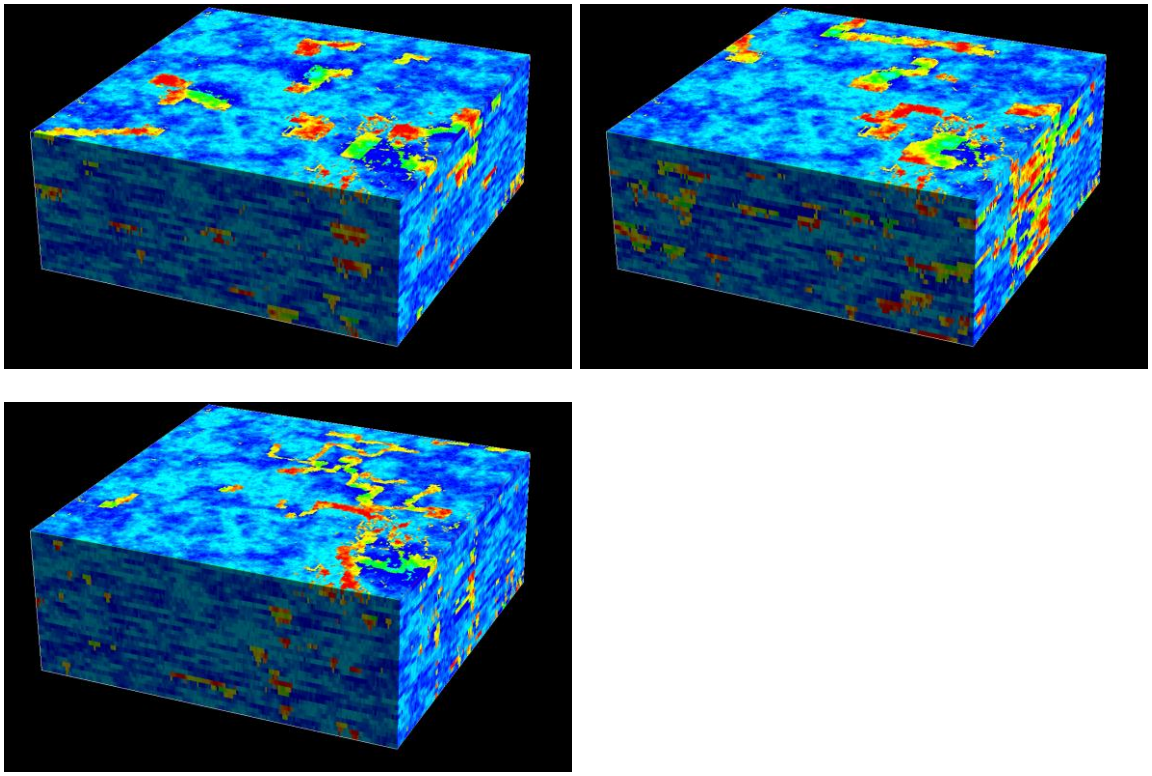

Figure 5.14 – Examples of three simulated images of porosity constrained to the morphology of the sand / shale system for 250 channels, 500 channels and 500 channels with half width.

5.6 Reservoir and potential OIP evaluation

The final step of modelling is application of porosity models for estimation of Potential Oil in Place (POIP). Curves of potential OIP are presented in the figure 5.15, 5.16 and 5.17 for each simulation scenario. These calculations demonstrate the applicability of the proposed methodology for the evaluation of reservoir reserves.

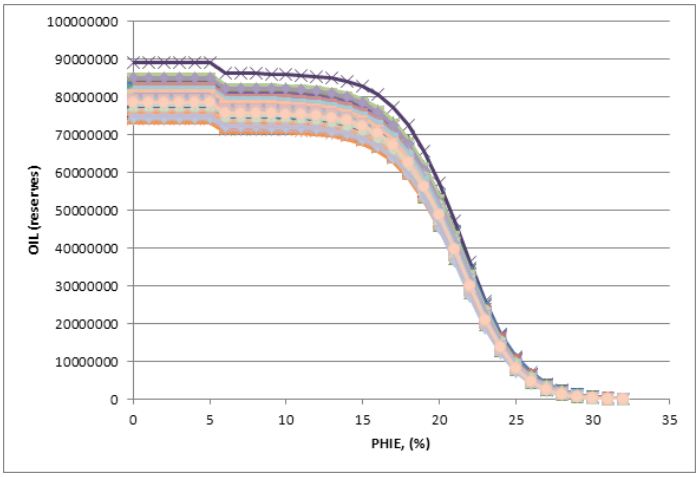

Figure 5.15 – Potential OIP curves the 250 channels scenario.

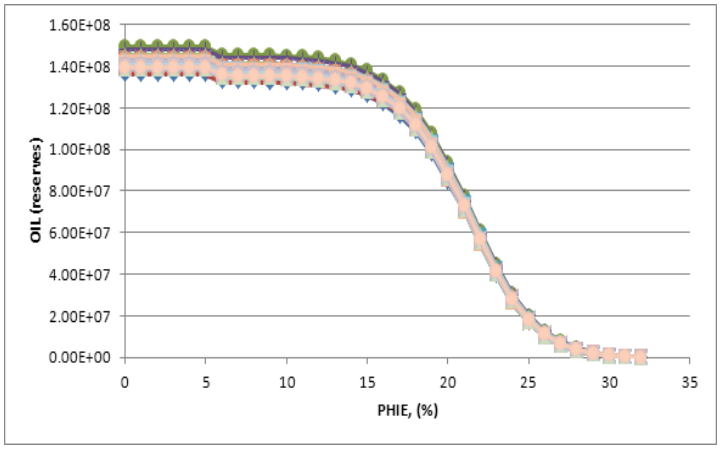

Figure 5.16 – Potential OIP curves the 500 channels scenario.

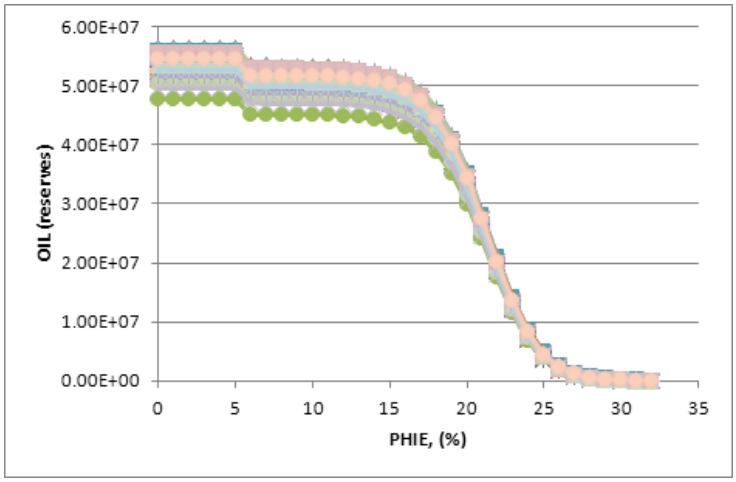

Figure 5.17 – Potential OIP curves the 500 channels, width /2 scenario.

5.7 Discussion

To discuss the results it is presented first a set of figures illustrating partial and final results in levels and cross-sections of the three scenarios (figures 5.18, 5.19 and 5.20)

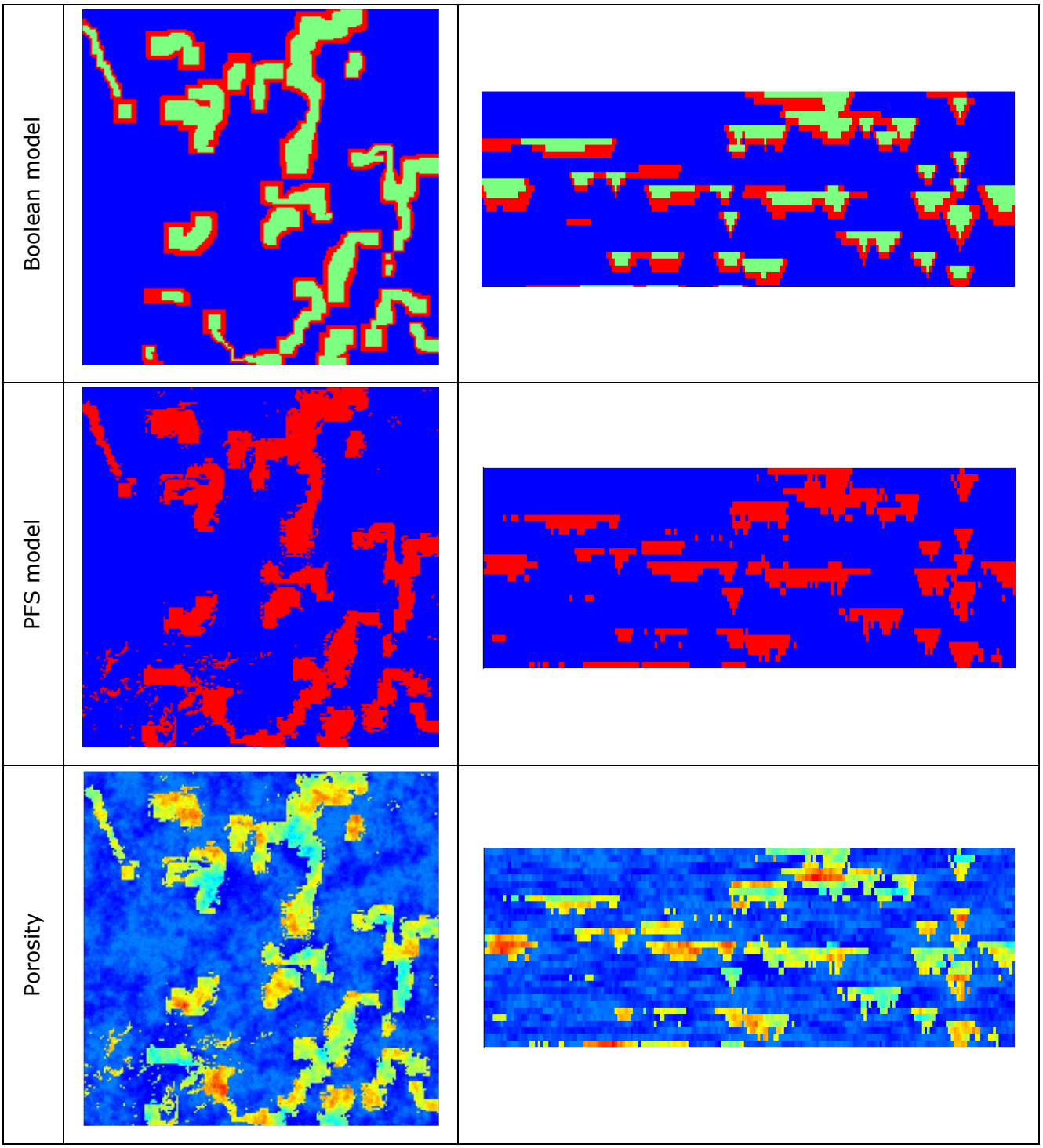

Figure 5.18 – Comparative results of one simulated image for (left) level and (right) cross-section for scenario of 250 channels.

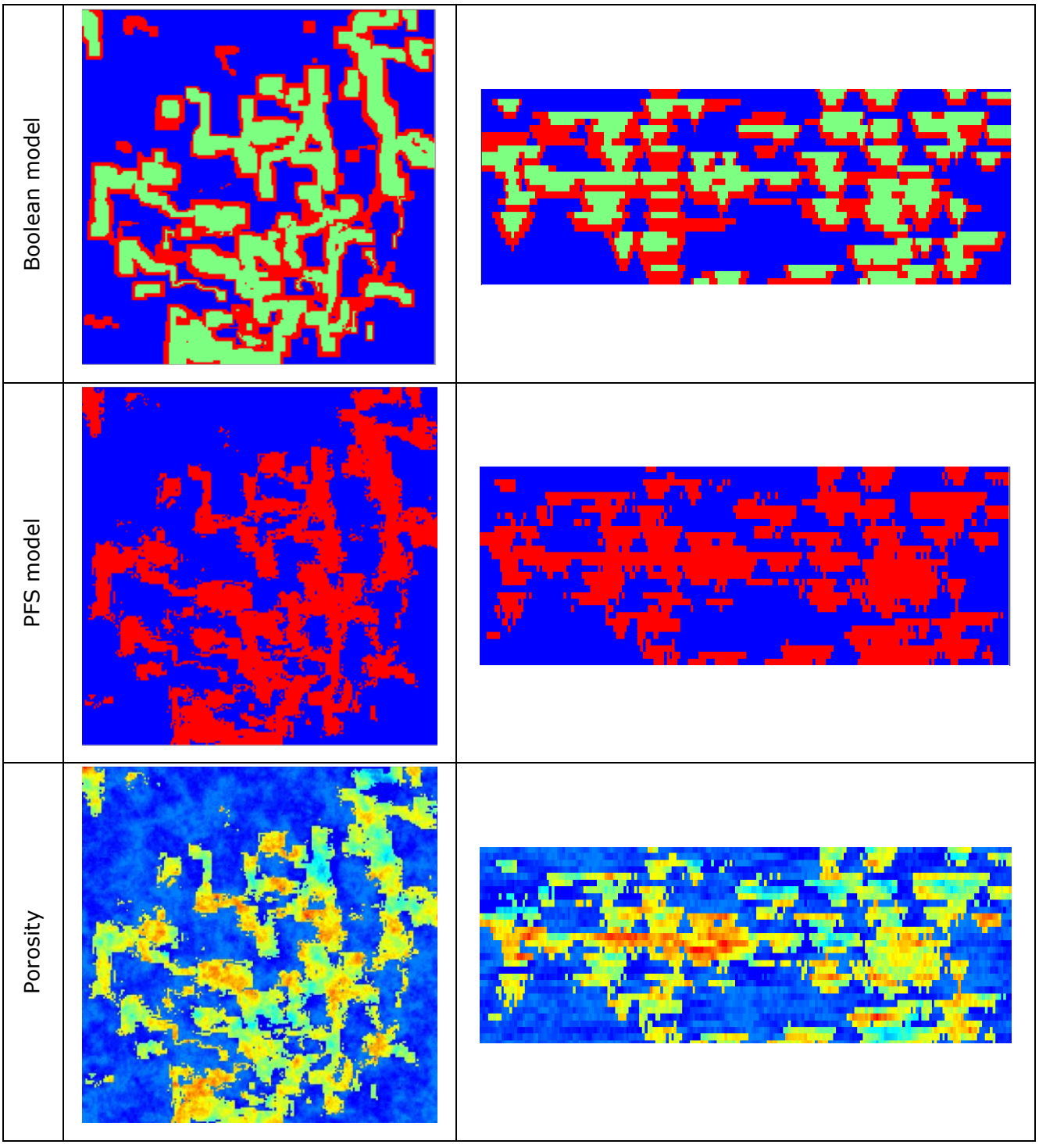

Figure 5.19 – Comparative results of one simulated image for (left) level and (right) cross-section for scenario of 500 channels.

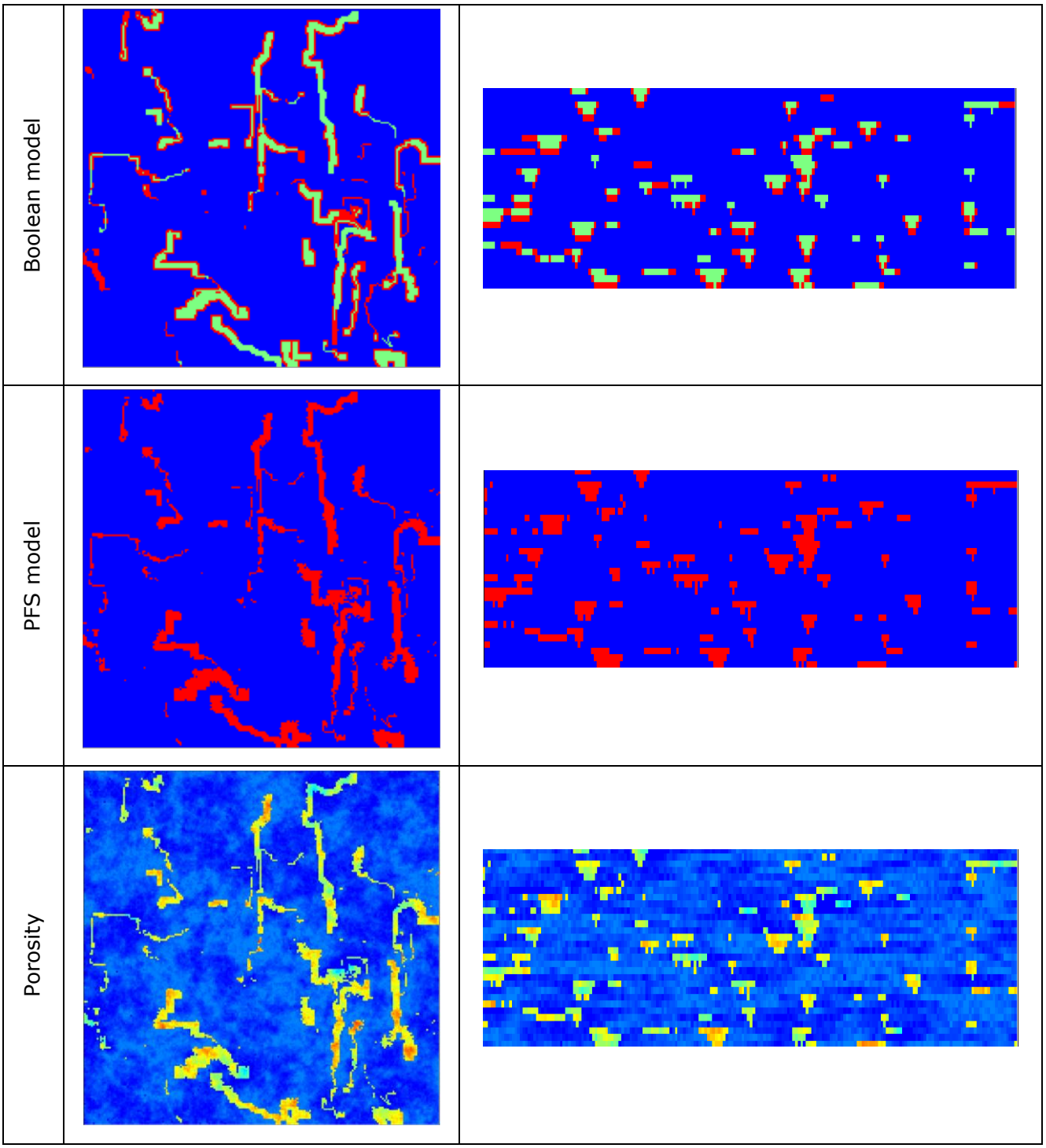

Figure 5.20 – Comparative results of one simulated image for (left) level and (right) cross-section for scenario of 500 channels and width / 2.

The sequence of results shows the follows:

Boolean model

a) From top to bottom, the shape of the channels is a half-ellipse.
b) Channels of the figure 5.8 are the same in number of the figure 5.7 but with half of the width, which is clearly observed.
c) Transition blocks in red are at both sides of the channel and at bottom. They were computed as 50% of the width and height.
d) The average length of the channels according the histogram of figure 5.1 is 2280m and the computed average of the simulated channels is always approximately 10% lower. This is explained because during growing process some channels reach the boundaries of the reservoir in both directions and therefore in these cases the total length of these channels is lower than the simulated from the histogram.
e) Channels vary in width and height according the simulated values showed in figure 5.4 and 5.5.
f) The entire network of channels follows from top to bottom the same orientation map which can be improved for realistic reservoirs if different images are taken into account in depth;
g) Proportions of each phase are similar for the different realizations (15). When the number of channels is multiplied by two (from 250 to 500), the proportion of sand are not multiplied by two, but for a factor lower which can be explained by the reservoir boundaries. When the width is subdivided by two the proportion of sands is much lower probably due to the approximation between the size of each block and the width of the channels.

PFS post-processing

a) Final simulated images follow the patterns of the Boolean models but the PFS post-processing (in average only 2% of the a priori shale and sand regions are converted to another) adds realism in the transition between shale and sands conditioned to a variogram model;
b) Statistics of the final simulated images are in accordance with the expected values obtained from the a priori probabilities from the PFS images (left columns of the tables 5.7, 5.8 and 5.9 and the a priori probability values of table 5.6). For instance for scenario of 500 channels, width /2:
   Channels proportion: 0,8454 x 0,02 + 0,0872 x 0,50 + 0,0674 x 0,98 = 0,1266 (0,1289)
   Sands proportion: 0,8454 x 0,98 + 0,0872 x 0,50 + 0,0674 x 0,02 = 0,8734 (0,8711)

Porosity

a) Simulated values of porosity are conditioned to sand and shale reference histograms via direct sequential simulation with local histograms;
b) Direct sequential simulation with local histograms enables the simulation of porosity for both facies in one unique step, instead of the two steps of the classical approach.

6. Final remarks

Recent news of searching alternative sources of energy show the critical situation of oil and gas industry: the majority of oil fields are in mature phases of exploitation (including enhanced oil recovery), others are located in extreme conditions (for instance, in off-shores at high depths), and therefore the prospection and exploitation requires more significant investments. In such conditions the only answer is to develop new modelling methodologies to deal with these new conditions.

In this work it was presented an innovative methodology of simulating 3D stochastic images of the morphology of fluvial sand channels reservoirs. For testing this methodology it was used synthetic data from a hypothetical channel sand reservoir and real porosity histograms from a Middle East reservoir. This type of reservoirs is a particular challenge for modelling, because of a complex geometry and sedimentological and structural heterogeneities.

In order to obtain a realistic model, the proposed methodology encompasses first the development of a Boolean or object model followed by a post-processing geostatistical algorithm (Probability Field Simulation). The combination of both algorithms enables to impose size statistics of the channels such as length, width and height and a variogram model. Moreover, the methodology generates a set of equally probable scenarios of the geometry of the sand / shale (channel / not channel) system. These morphological images can be, in a second step, filled with petrophysical properties values, such as porosity and permeability. For illustration purposes, porosity was generated by Direct Sequential Simulation with local histograms of the two regions. The final step of modelling was application of porosity models for estimation of Potential Oil in Place (POIP). These calculations demonstrate the applicability of the proposed methodology for the evaluation of reservoir reserves.

The obtained results for three scenarios of channels (low density, high density, and high density with thin channels) showed advantages relatively to other methods:

a) Boolean model impose statistics of shape (half-ellipse section), sizes and local orientation in a very efficient way;
b) Post-processing by Probability Field Simulation transforms the previous morphology according a variogram model adding realism;
c) Implementation of the Direct Sequential Simulation with local histograms enables the simulation of properties for both facies in one unique step, instead of the two steps of the classical approach.

7. REFERENCES

Almeida, A., Journel, A., 1994. Joint simulation of multiple variables with a Markov-type corregionalization model. Mathematical geology 26(5): 565-588.

Almeida, J.A., 1999. Use of geostatistical models to improve reservoir description and flow simulation in heterogeneous oil fields. PhD thesis IST - 161.

Almeida, J.A., Barbosa, S. 2008. 3D stochastic simulation of fracture networks conditioned both to field observations and a linear fracture density. Proceedings of the eighth international geostatistics congress, Santiago do Chile: 129-136.

Almeida, J.A., 2010. Stochastic simulation methods for characterization of lithoclasses in carbonate reservoirs. Earth Science Reviews, (101), 3-4: 250-270.

Basic Petroleum Geology and Log Analysis, 2001, Hallibuton: 28-32.

Compton, R.R., 1985. Geology in the Field. John Wiley and Sons, New York - 398.

Deutsch, C.V., Journel, A., 1992. GSLIB: Geostatistical Software Library and User's Guide. Oxford University Press, Stanford.

Deustch, C.V., Wang, L., 1996. Hierarchical object based stochastic modeling of fluvial reservoirs. Mathematical Geology, v. 28:857-880.

Eaves E., 1976. Citronelle oil field, Mobile country, Alabama. Am Assos Petrol Geol Mem 16: 259-275.

Elliot L., 1989. The Surat and Bowen basins. Aust Petrol Explor Assoc J 29: 398-416.

Fritz, W., Moore, J., 1988. Exercises in Physical Stratigraphy and Sedimentology. John Wiley and Sons, USA - 221.

Froidevaux, R., 1993. Probability Field Simulation, in A. Soares (ed), Geostatistics Troia'92, Kluwer Academic Pub., Dordrecht, 1: 73-84.

Goovaerts, P., 1997. Geostatistics for Natural Resources Evaluation. Oxford University Press, New York - 483.

Holden, L., Hauge, R., Skare, O., Skorstad, A., 1998. Modeling of fluvial reservoirs with object models. Mathematical Geology, 30: 473-496.

Hu, L.Y., Chugunova, T., 2008. Multiple-point geostatistics for modeling subsurface heterogeneity: a comprehensive review. Water Resources Research; 44: W11413.

Keogh, K., 2007. Sequence stratigraphy and 3-D modelling of the East Pennine Coalfield, UK: a deterministic and stochastic approach. PhD thesis, University of Liverpool, UK - 281.

Leeder, M., 1999. Sedimentology and Sedimentary Basins: from turbulence to tectonics. Blackwell Science Ltd - 592.

Lorenz J.C., Warpinski N.R., Branagan P.T., 1991. Subsurface characterization of Mesaverde reservoirs in Colorado: geophysical and reservoir-engineering cheks on predictive sedimentology. Soc Econ Paleontol Mineral Conc Sedimentol Paleontol 3: 57-79.

Luis, J., Almeida, J.A., 1997. Stochastic Characterization of Fluvial Sand Channels, Geostatistics Wollongong'96, Volume 1, eds. E. Y. Baafi and N. A. Schofield. Kluwer Academic Publ., Netherlands: 477-488.

Lyons P.L., Dobrin M.B., 1972. Seismic exploration for stratigraphic traps. Am Assos Petrol Geol Mem 16:225-243.

Mariethoz, G., Kelly, B.F.J., 2011. Modelling complex geological structures with elementary training images and transform-invariant distances. Water Resources Research; 47: W07527.

Mata-Lima, H., 2008. Reservoir characterisation with iterative direct sequential co-simulation: integrating fluid dynamic data into stochastic model. Journal of Petroleum Science and Engineering doi: 10.1016/j. petrol.2008.07.003.

Matheron G., Beucher H, Fouquet, C., Galli A., Guerrilot D., Ravenne C., 1987. Conditional simulation of the geometry of fluvio-deltaic reservoirs. In: SPE Annual Technical Conference and Exhibition, 62, Dallas-TX: 123-130, SPE #16753.

Miall, A., 1996. The geology of fluvial deposits: sedimentary facies, basin analysis, and petroleum geology. Springer-Verlag Berlin Heidelberg - 582.

Neuendorf, K., Mehl, J., Jackson, J., eds., 2005. Glossary of Geology. American Geological Institute. Alexandria, Virginia - 800.

North, F., 1985. Petroleum Geology, University Press, Cambridge.

Nunes, R., Almeida, J.A., 2010. Parallelization of sequential Gaussian, indicator and direct simulation algorithms. Computers & Geosciences, vol. 36: 1042-1052.

Peredo, O., Ortiz, J.M., 2011. Parallel implementation of simulated annealing to reproduce multiple-point statistics. Computers and geosciences. 37: 1110-21.

Reading, H., 1996. Sedimentary Environments: Processes, Facies and Stratigraphy. Department of Earth Sciences, University of Oxford, Third Edition - 688.

Reynolds D.W., Vincent J.K., 1972. Midland gas field, western Kentucky. Am Assos Petrol Geol Mem 16:585-598.

Roxo, S., 2011. Integração de informação secundária na modelação geoestatistica da qualidade de solos em locais potencialmente contaminados. Aplicação à área subjacente de uma antiga refinaria. MsC Thesis. FCT-UNL - 64.

Soares, A., 1990. Geostatistical estimation of orebody geometry: morphological kriging. Mathematical Geology 22(7): 787-802.

Soares, A., 2001. Direct Sequential Simulation and Cosimulation. Mathematical Geology, 33(8): 911–926.

Soares, A., 2006. Geoestatística para as Ciências daTerra e do Ambiente. IST Press - 214.

Srivastava, M., 1992. Reservoir Characterization with Probability Field Simulation, *SPE Paper*, N. 24753.

Strebelle, S., 2002. Conditional simulation of complex geological structures using multiple-point geostatistics. Mathematical Geology. 34: 1-22.

Vargas-Guzmnan, J., Al-Qassab, H., 2006. Spatial conditional simulation of facies objects for modelling complex clastic reservoirs. Journal of Petroleum Science and Engineering 54 (1-2): 1-9.

Weber, K.J., 1986. How heterogeneity affects oil recovery. Academic Press: 487-566.

Weber, K.J., Van Geuns L.C., 1990. Framework for constructing clastic reservoir simulation models. J Petrol Technol 42: 1248-1253.

Wilson, W., Moore, J., 2003. Glossary of Hydrology. American Geological Institute, Springer - 248.

Woncik J., 1972. Recluse field, Campbell Country, Wyoming. Am Assos Petrol Geol Mem 16:376-382.

Wood J.M., Hopkins J.C., 1992. Traps associated with paleovalleys and interfluves in an unconformity bounded sequence: Lower Cretaceous Glauconitic Member, southern Alberta, Canada. Am Assoc Petrol Geol Bull 76: 904-926.

Yinan Q., Peihua X., Jingsiu X., 1987. Fluvial sandstone bodies as hydrocarbon reservoirs in lake basins. Soc Econ Paleontol Mineral Spec Publ 39:329-342.